

Review

TM-Free and TM-Catalyzed Mechano-synthesis of Functional Polymers

Wahab K. A. Al-Ithawi^{1,2}, Albert F. Khasanov¹ , Igor S. Kovalev¹ , Igor L. Nikonov^{1,3} , Vadim A. Platonov¹, Dmitry S. Kopchuk^{1,3}, Sougata Santra¹, Grigory V. Zyryanov^{1,3,*} and Brindaban C. Ranu^{1,4}

¹ Chemical Engineering Institute, Ural Federal University, 19 Mira St., 620002 Yekaterinburg, Russia

² Energy and Renewable Energies Technology Center, University of Technology—Iraq, Baghdad 10066, Iraq

³ I. Ya. Postovsky Institute of Organic Synthesis of RAS (Ural Division), 22/20 S. Kovalevskoy/Akademicheskaya St., 620219 Yekaterinburg, Russia

⁴ School of Chemical Sciences, Indian Association for the Cultivation of Science, Jadavpur, Kolkata 700032, India

* Correspondence: gvzyryanov@gmail.com; Tel.: +7-(343)-375-4501

Highlights:

- The most representative examples for the TM-free and TM-catalyzed mechano-synthesis of functional polymers are reported;
- The most common applications for the various types of functional polymers are presented;
- The advantage of solvent-free mechano-synthesis over conventional solvent-based synthesis are highlighted;
- In many cases the better performance of the mechanochemically-prepared polymers over those obtained by using conventional methods are demonstrated.



Citation: Al-Ithawi, W.K.A.; Khasanov, A.F.; Kovalev, I.S.; Nikonov, I.L.; Platonov, V.A.; Kopchuk, D.S.; Santra, S.; Zyryanov, G.V.; Ranu, B.C. TM-Free and TM-Catalyzed Mechano-synthesis of Functional Polymers. *Polymers* **2023**, *15*, 1853. <https://doi.org/10.3390/polym15081853>

Academic Editors: Sumant Dwivedi, Mohamad Al-Sheikhly and Placido Mineo

Received: 10 March 2023

Revised: 4 April 2023

Accepted: 7 April 2023

Published: 12 April 2023

Abstract: Mechanochemically induced methods are commonly used for the depolymerization of polymers, including plastic and agricultural wastes. So far, these methods have rarely been used for polymer synthesis. Compared to conventional polymerization in solutions, mechanochemical polymerization offers numerous advantages such as less or no solvent consumption, the accessibility of novel structures, the inclusion of co-polymers and post-modified polymers, and, most importantly, the avoidance of problems posed by low monomer/oligomer solubility and fast precipitation during polymerization. Consequently, the development of new functional polymers and materials, including those based on mechanochemically synthesized polymers, has drawn much interest, particularly from the perspective of green chemistry. In this review, we tried to highlight the most representative examples of transition-metal (TM)-free and TM-catalyzed mechano-synthesis of some functional polymers, such as semiconductive polymers, porous polymeric materials, sensory materials, materials for photovoltaics, etc.

Keywords: functional polymers; ball-milling; green chemistry; solid-state chemistry; solvent-free synthesis; TM-catalyzed synthesis; TM-free synthesis



Copyright: © 2023 by the authors. Licensee MDPI, Basel, Switzerland. This article is an open access article distributed under the terms and conditions of the Creative Commons Attribution (CC BY) license (<https://creativecommons.org/licenses/by/4.0/>).

1. Introduction

According to the International Union of Pure and Applied Chemistry (IUPAC), among the 10 chemical innovations that could impact society, reactive extrusion could be the most promising one as it allows chemical reactions to be carried out completely in solvent-free conditions with good E-factors and, thus, with a lower negative impact on the environment [1]. One remarkable example of such a technique is the use of mechano-synthesis, such as grinding, ball-milling etc., as an equal or, in most cases, better alternative to conventional solvent-based conditions for carrying out chemical reactions. In turn,

a most remarkable example of such reactions is solvent reduced or solvent-free polymerization, including processes involving coordination bonds [2] under mechanochemical, most commonly ball-milling, conditions. Therefore, the methods for making polymers under grinding/ball-milling conditions, which were formerly used to rupture them, are of wide interest in the chemical community worldwide [3].

It worth mentioning that in past decades, mechanochemical processes/reactions have attracted growing attention due to the green aspects of this type of synthesis [4], especially for the utilization of recyclable materials [5,6], the preparation of biologically active compounds [7,8], the preparation of various types of polymers [9], and the other types of materials [10,11].

In this review, the most representative examples of the mechanochemical synthesis of functional polymers are presented. The obtained polymers are arranged according to their possible applications and/or polymerization conditions.

2. Results and Discussion

2.1. Mechanochemical Synthesis of Conductive Polymers

The high electrical conductivity of polyacetylenes and polyethylenes were discovered for the first time in the 1970s [12], and since that time these polymers have become promising materials for molecular electronics [13–16]. On the other hand, poly(*p*-phenylene vinylenes) (PPVs) possess several of such extraordinary attributes, such as tunable optical properties, good reactivity, and high electrical conductivity [17], and, therefore, they are considered as advanced materials for electronics applications, particularly for OLEDs [18]. In 2014, Swager's group reported the mechanochemical synthesis of poly(phenylene vinylene) [19] (Figure 1). To achieve this, the authors used solid-state base-catalyzed Gilch polymerization in a Retsch vibrational mill and zirconium oxide jar/milling balls. Depending on the amount of milling time, base strength, solid-state dilution, milling frequency, and the size of the milling balls, various polymerization degrees were observed. In the most representative case, PPVs up to a 40 kDa molecular weight were prepared in up to a 70% yield after 30 min milling with 6 eq. of KOtBu. Polymer molecular weights and polydispersity indices were estimated by gel permeation chromatography (GPC) using polystyrenes as standards.

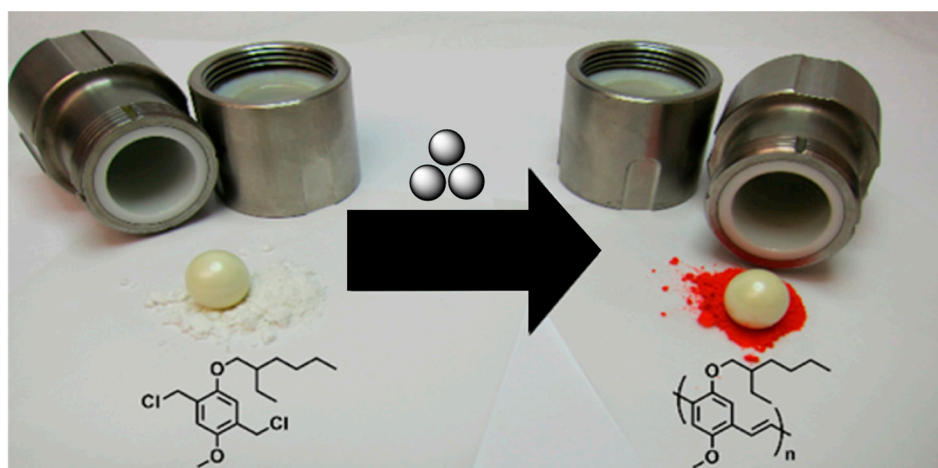


Figure 1. Ball-milling approach to PPVs. Reproduced with the permission of reference [19].

Among semiconductive polymers, polypyrroles (PPy) are the most attractive ones due to their high conductivity, good stability, and great applicability for various tasks, such as energy storage and transfer, sensory applications [20–23], and functional membranes [24–26]. Electrochemical or chemical oxidative polymerization in water or organic solutions is a common way to prepare polypyrroles. Depending on the type of oxidant and solvent, polypyrroles of various conductivities can be obtained [27,28]. For instance, in an aqueous

medium in the presence of ammonium persulfate, PPy with a conductivity not higher than $0.5 \text{ S}\cdot\text{cm}^{-1}$ was obtained [29].

Posudievsky and Kozarenko [30] reported the synthesis of PPy by using solvent-free ball-milling in the presence of ammonium persulfate as an oxidant at an uncommon (for solvent-based approaches) value of the monomer/oxidant (ammonium persulfate) mole ratio equal to two. The PPy was obtained in a high yield, and the greatest level of conductivity ($6.5 \text{ S}\cdot\text{cm}^{-1}$) was achieved.

In a later study [31], the same authors proposed the formation of highly conducting PPy at a high monomer/oxidant (ammonium persulfate) mole ratio via the chain mechanism with the intermediate formation of poly(3-pyrroline) and its further mechanochemical dehydrogenation via both an oxidative (ammonium persulfate) method and under the action of mechanical forces. For the obtained PPy, a conductivity above $5 \text{ S}\cdot\text{cm}^{-1}$ was achieved only at a relatively low oxidant content in the initial reaction mixture. Based on the TEM data, the PPy with the highest conductivity consisted of up to $\sim 100 \text{ nm}$ nanoparticles with a core-shell structure, with the material of the shell being amorphous and the core being formed by more closely packed polymer macromolecules.

2.2. Mechanochemistry of Polystyrenes and Poly(2-vinylnaphthalene)

Polystyrene (PS) and poly(2-vinylnaphthalene) (PVN) are known to exhibit excimer-induced energy migration properties [32,33], strong excimer fluorescence, and phosphorescence [34,35]. In addition, they are important components for plastic scintillators [36–39].

Cho and Bielawski published a paper on the mechanochemistry of PVN (Figure 2) by using a variant of atom transfer radical polymerization under ball-milling conditions using 2-vinylnaphthalene, phenylethyl bromide (initiator), and $\text{CuI}/\text{Br}/\text{tris}(2\text{-pyridylmethyl})\text{amine}$ (catalyst) under nitrogen using 10 mm diameter zirconium dioxide jar/balls in a vibrational ball mill at 30 Hz for 6 h [40]. By using semi-logarithmic plot of the monomer concentration vs. time, a linear dependence was observed, with the conversion of the polymerization reaction reaching as high as 97 % after 6 h. In addition, a linear correlation between the polymer MW and monomer conversion was observed, although the experimental M_n , which was estimated by means of size-exclusion chromatography (SEC) using anisole as a standard, was in fact lower than the theoretical one, which was possibly due to premature mechanical degradation.

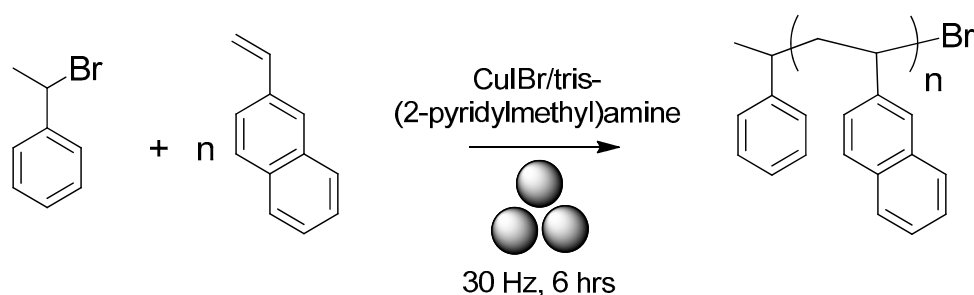


Figure 2. Mechanochemistry of PVN.

It is worth mentioning that at a frequency of 10 Hz for 6 h and at the same reagents ratio, no significant polymerization was observed, while at a frequency of 20 Hz, the formation of the desired polymer took place with an M_n of 16.0 kDa, although with a monomer conversion of 50 % and a relatively broad polydispersity (Đ of 3.23). The monomer conversion was analyzed by ^1H NMR spectroscopy.

In 2007, Hasegawa and co-authors reported the mechanochemically initiated polymerization of styrene via its grinding with talc in SiN_3 jar/milling balls (8.5 mm) at 24 Hz in a vibrating ball mill [41]. The obtained PSs were isolated as composites of talc particles, that is, the polymer was attached to the talc particles. Their time-conversion studies demonstrated that the polymerization of styrene took place within 1 h, and the conversion of

styrene depended strongly on either the grinding time or talc concentration. For instance, a 41% conversion was observed at a talc concentration of 15 wt% with a grinding time of 6 h, while only a 50% conversion was observed after 24 h. The molecular weight of the polymers was measured by means of GPC, and the highest M_n observed was 1.6×10^6 Da. Thus, the authors suggested an efficient way toward forming clay nanocomposites composed of widely used polystyrene possessing attractive thermomechanical properties.

Very recently, Kim and co-authors reported a mechanochemical solid-state vinyl polymerization method [42] (Figure 3). In their study, either 4-vinyl biphenyl or 4-biphenyl methacrylate in zirconia jars/milling balls (8 mm) were subject to ball-milling in a Retsch Mixing Mill MM400 at 30 Hz for 1 h to produce **BPP1-2** polymers with a 99% conversion. It worth mentioning that at lower speed lower or no conversion was observed.

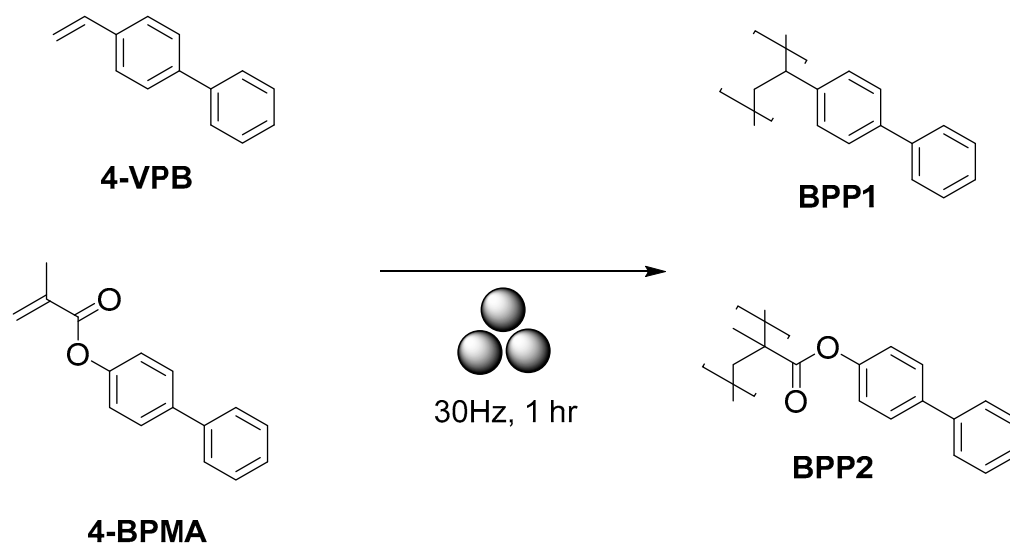


Figure 3. The mechanochemical synthesis of biphenyl-appended polymers.

The same polymerization was also carried out by using an anionic initiator, such as *sec*-BuLi. According to the authors, the alkyl-anion-promoted polymerization proceeded with excluding radical initiation, and the generally expected features of anionic polymerization, such as molecular weight control and narrow dispersity, were not observed (PDI = 1.25–4.46, M_w = 23.5–309 kDa). The molecular weights of the polymers were determined by SEC analysis using polystyrenes as standards, and the conversion degree was determined by ^1H NMR spectroscopy. It was suggested that upon ball-milling, the mechanical force fractured the newly formed polymer chains via anionic initiation to generate macroradicals, and these newly formed radicals participated in the polymerization process. In other words, the anionic process was responsible for only the initiation step, and after that, the ball-milling made the radical process become dominant during the polymerization.

2.3. Mechanochemical Synthesis of Polyazomethines

The main difference in polyazomethines (PAMs) from polyacetylenes is the presence of C=N moieties, which are isoelectronic to CH=CH ones, and they both have a similar planar molecular structure and maximum absorption peak. Owing to the much easier formation of C=N bonds, PAMs can be suitable alternatives to polyacetylenes. PAMs are widely used in optoelectronic devices [43] such as photovoltaic cells [44,45], electroluminescent devices [46], and electrochromic devices [47–49]. Importantly, the dynamic nature of azomethine bonds provides new avenues for using polyazomethines as components for biocompatible and totally disintegrable electronics [50]. However, as with most high-molecular-weight conjugated polymers, the low solubility of polyazomethines in common organic solvents limits their preparation, processability, characterization, and application.

Therefore, the mechanochemistry of PAM is a good alternative to conventional solution-based procedures.

In 2016, Grätz and Borchardt reported [51] the very-first mechanochemical approach to polyazomethines, **PAM1**, by mixing equal molar amounts of *p*-phenylenediamine and terephthalic aldehyde in a zirconium oxide milling cup with 22 zirconium oxide milling balls (d10 mm) at 800 rpm for 45 min to produce the desired polymer with $M_n = 3010$ Da and PDI = 1.36 (based on the data of MALDI-TOF) (Figure 4):

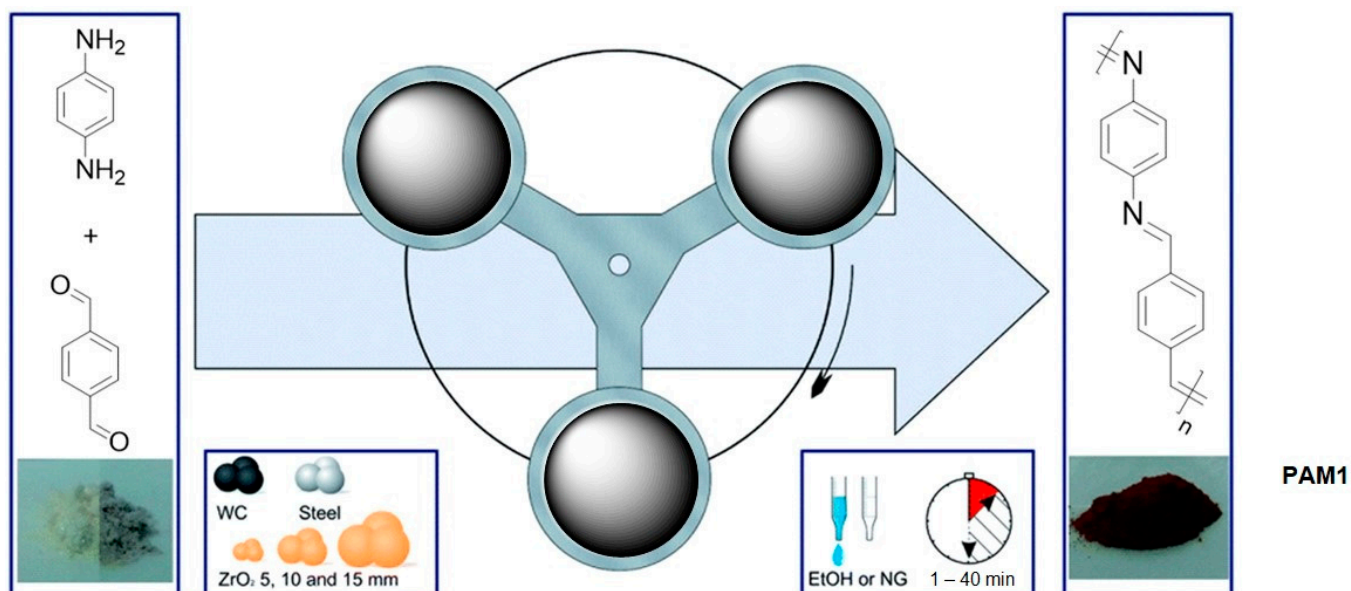


Figure 4. The mechanochemistry of **PAM1**. Reproduced with the permission of reference [51].

According to the authors, the obtained polymers had a high thermal stability and low optical bandgaps ($\lambda_{\max} = 456$ nm). The influence of the milling ball size and material was investigated, and the tungsten carbide ones gave the highest conversion, but all the materials gave higher yields compared to solution polymerization due to the absence of the influence of the solvent. The formation of **PAM1** could be easily monitored by solid-state IR based on the appearance of a vibration of the C=N group at 1609 cm^{-1} as well as the disappearance of the vibrations of the carbonyl and amine groups at 1686 cm^{-1} and 1514 cm^{-1} , respectively. All the above-mentioned information strongly supports the effectiveness of mechanochemistry for the preparation of polyazomethines.

We recently reported on the mechanochemical synthesis of diketo-pyrrolopyrroles (DPPs)-based azomethine polymers [52] (Figure 5). Two synthetic strategies were used. In the first approach, a combination of Pd(OAc)₂-catalyzed Suzuki cross-coupling and a condensation reaction was used, and dibromo-substituted **DPPBr** reacted with 4-(4,4,5,5-tetramethyl-1,3,2-dioxaborolan-2-yl)aniline and terephthalic aldehyde in the presence of potassium carbonate in a stainless-steel jar/milling balls upon ball-milling in a Retch Planetary Mill PM100 at 500 rpm for 4 h to produce the polymer **PAM2** in a 60% yield. In the second approach, owing to the wide use of DPP-based materials for biological applications [53], a cytotoxic Pd-free synthesis was developed by reacting aniline-appended **DPPNH₂** with terephthalic aldehyde in the presence of *p*-toluenesulphonic acid (*p*-TSA) and with an excess of CaCl₂ as a dehydrating agent to produce target polymer **PAM2** in a yield as high as 85%.

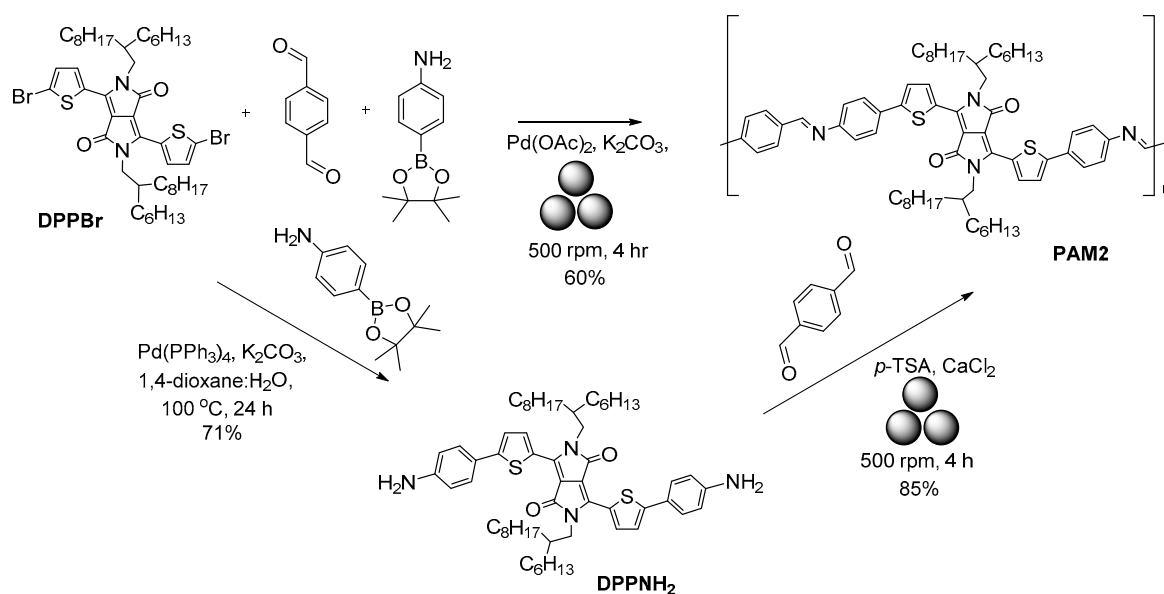


Figure 5. The mechanosynthesis of DPP-based polyazamethine, **PAM2**.

By using similar conditions, an azamethine-linked dibenzo[*a,c*]phenazine-containing polymer **PAM3** was prepared [54] (Figure 6). The $M_n = 5365$ Da was calculated by using ^1H NMR end-group analysis.

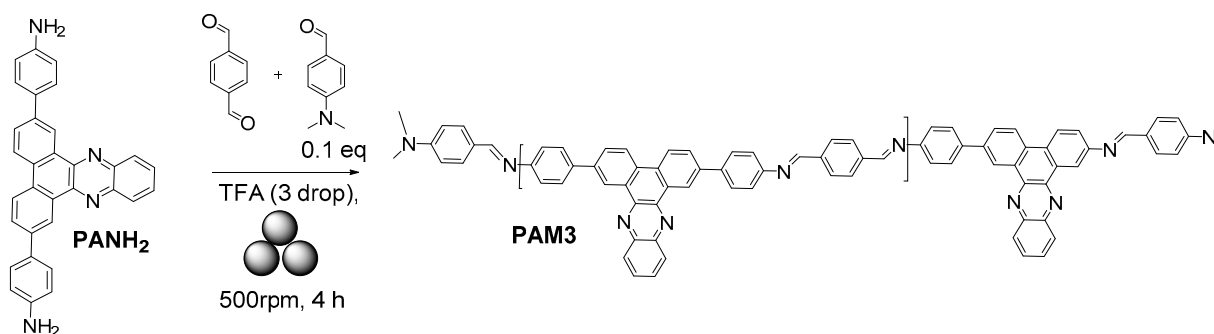


Figure 6. The mechanosynthesis of dibenzo[*a,c*]phenazine-containing polymer, **PAM3**.

2.4. Mechanosynthesis of Biopolymers and (Bio)Degradable Polymers

In past decades, closed-loop plastic recycling, as a process by which a product or material can be used and then turned into a new product or converted back to raw material without losing its properties during the recycling process, has gained wide interest worldwide [55–63]. For instance, dynamic covalent polymers, such as vitrimers, have been proposed as a possible alternative to non-recyclable polymers [64–70]. It is worth mentioning that the depolymerization of vitrimers is still a challenge as it commonly requires high temperatures and, in many cases, it does not produce the starting monomers but produces short oligomers.

Christensen et al. suggested using diketoenamine dynamic bonds and mechanical force for the closed-loop recycling of plastic poly(diketoenamine)s (PDKs) [71]. In their work, **PDK1-3** was prepared in high yields (95%) via simple polycondensation reactions between β -triketones and either aromatic or aliphatic amines by using a stainless-steel jar/milling balls in a SPEX SamplePrep 8000 Mixer/Mill for between 15 and 60 min (Figure 7).

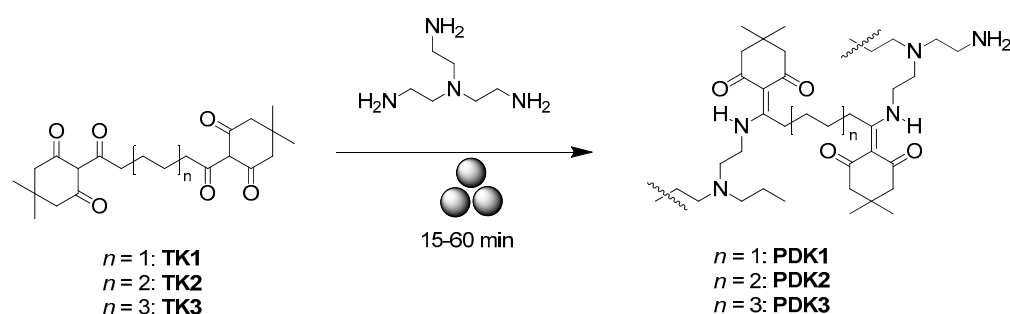


Figure 7. The mechanochemical synthesis of poly(diketoenamine)s PDK1-3.

In addition, the authors reported a recycling process (depolymerization) for the polymer to recover the used monomers. A disintegration process occurred during room-temperature hydrolysis in aqueous strong acid solutions to collect pure triketones, while the amine monomers were recovered by a regenerative resin-based process. Interaction with sulfuric or hydrochloric acids (5.0 M) during 12 h recovered the pure monomers in a more than 90% isolated yield. Moreover, it was confirmed experimentally that the presence of various types of polymers and plastics, such as poly(ethylene terephthalate) (PET), nylon-6,6 (PA), polyethylene (PE), poly(vinyl chloride) (PVC), and polycarbonate (PC), as well as dyes, inorganic substances, etc., did not interfere with the regeneration process, thus confirming the high ability of PDKs to be recovered in a high selectivity. This degradation/regeneration process represents an efficient closed-loop recycling method of a polymer with potential applications in biodegradable materials.

Poly(lactic acid)(PLA)-based polymers are another type of readily degradable materials for bioplastics [72]. In 2019, Lee and co-workers reported the mechanochemical synthesis of PLA block copolymers [73] (Figure 8).

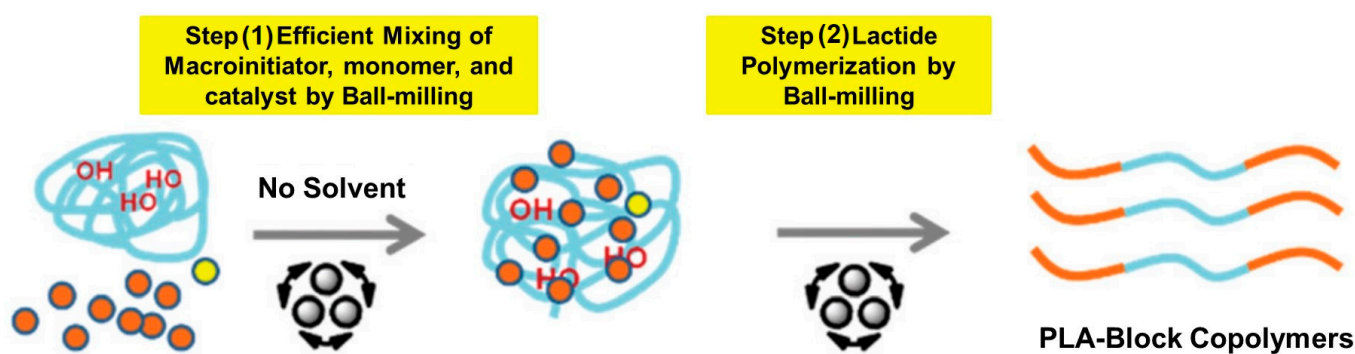


Figure 8. The mechanochemical synthesis of poly(lactic acid) block co-polymers. Reproduced with the permission of reference [73].

In the most representative case, the authors were able to prepare PLA-PEO-PLA block copolymer via the reaction of *D*-Lactide, polyethylene oxide 6000, and DBU in a stainless-steel milling container/milling ball (12 mm diameter) in a Retsch Mixer Mill MM 400 at 20 Hz for 1 h to produce the target polymer with $M_n = 17.9$ kDa (PDI = 1.33, based on GPC) with a >99% conversion. By using a similar approach (7 mm milling ball), other di- and three-block co-polymers, such as PLA4000-P ϵ DL4600-PLA4000 (92%, 19.9 kDa, PDI = 1.52), PLA4000-P δ DL4400-PLA4000 (88%, 10.7 kDa, PDI = 1.41), P ϵ CL4800-PLA4000 (89%, 11.3 kDa, PDI = 1.20), PLA2000-PTHF2900-PLA2000 (94%, 8.89 kDa, PDI = 1.55), and PLA4000-PTHF2900-PLA4000 (83%, 13.2 kDa, PDI = 1.26), were successfully prepared. Due to the biodegradability of PLA, these polymers could have biomedical applications.

Along with 2,5-furandicarboxylic acid (FDCA) [74,75] and 5-hydroxymethylfurfural (HMF) [76], 2,5-bis(hydroxymethyl)furan (BHMF) can be considered as one of the important bio-based building blocks for green chemistry and as an important monomer for

biopolymers. In 2020, Oh and co-authors [77] reported a facile mechanochemical synthesis of BHMf-derived eco-friendly polyurethanes (PUs) (Figure 9). To achieve this, BHMf was reacted with di-isocyanates in the presence of either DBTDL, DABCO, or DBU upon ball-milling in a vibration mill. As a result of these two-component mechanochemical polymerization reactions, a variety of BHMf-containing PUs were obtained with a Mw that varied from 5 to 163 k with PDI = 1.18–2.75. According to the authors, these PUs were flexible ($T_g = 96\text{ }^\circ\text{C}$) and thermally stable ($T_d = 197\text{ }^\circ\text{C}$). In addition, three-component mechanochemical polymerization was carried out (with BHMf and equimolar amounts of either aliphatic diols or diamines) to produce PU co-polymers with a wide variation in the polymer properties, such as the glass transition temperature and molecular weight ($M_w = 13\text{--}111\text{ kDa}$, PDI = 1.25–1.75).

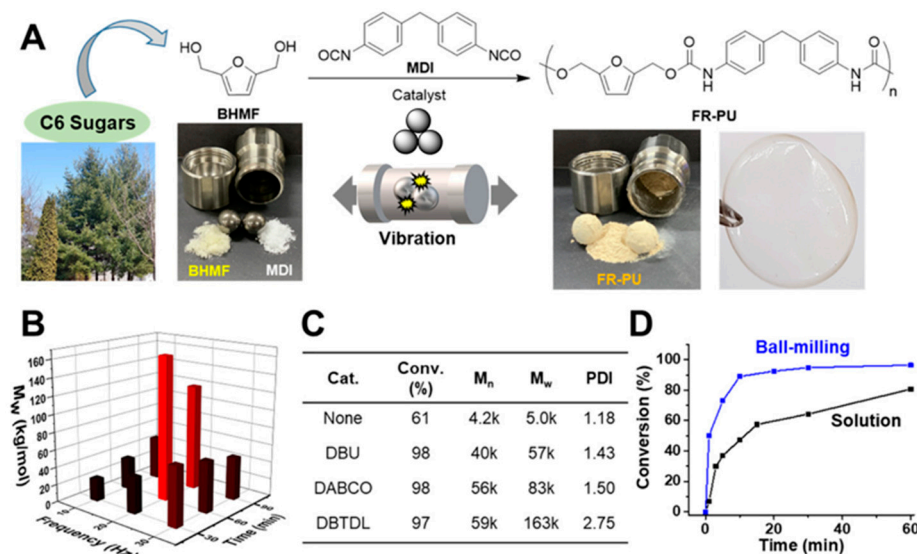


Figure 9. (A) Schematic illustration of PU synthesis using diols derived from biomass. Screening of ball-milling polymerization with BHMf and MDI (B) by controlling the frequency and the reaction time and (C) with several catalysts. The reaction with the DBTDL catalyst at 20 Hz for 60 min yielded the highest Mw PU. (D) Comparison of conversion achieved with ball-milling vs. solution synthesis of PU as a function of the reaction time. Reproduced with the permission of reference [77].

2.5. Mechanochemical Synthesis of Polyphenylenes

Functional polyphenylenes (FPPs) are one of the hottest topics for use in organic electronics [78,79] and photovoltaics [80]. The most common methods for the preparation of FPPs involve the Friedel–Crafts [81], Ullmann, and Suzuki cross-coupling reactions. However, the low solubility of FPPs is the main drawback for their preparation by solvent-based methods. Therefore, some synthetic approaches, such as polymerization on a surface [82] and Friedel–Crafts post-modification [83], are used.

Borchardt's group reported a series of works on mechanochemical Suzuki cross-coupling polymerization [84,85] (Figure 10). In the most representative case, 1,4-dibromobenzene reacted with 1,4-phenyldiboronic acid in the presence of palladium acetate and potassium carbonate in a zirconium oxide jar with 22 zirconium oxide grinding balls (10 mm) in a Fritsch Pulverisett 7 planetary ball mill at 800 rpm for 30 min to afford the linear polyphenylene (FPP1) with an outstanding degree of polymerization (DP) of 164. Among all the aryl halides used, bromide was found to be the best functional group, leading to the highest DP and yield while also showing a defined structure of the polymers. According to the authors, the atom economy of the Suzuki reaction (38%) was identical for conventional solvent-based and mechanochemical approaches. However, the conventional solvent-based process proceeded with low mass productivity of 1.4% (due to the solvents present). Finally, the mechanochemical approach provided three-times-as-high yields (10.6%).

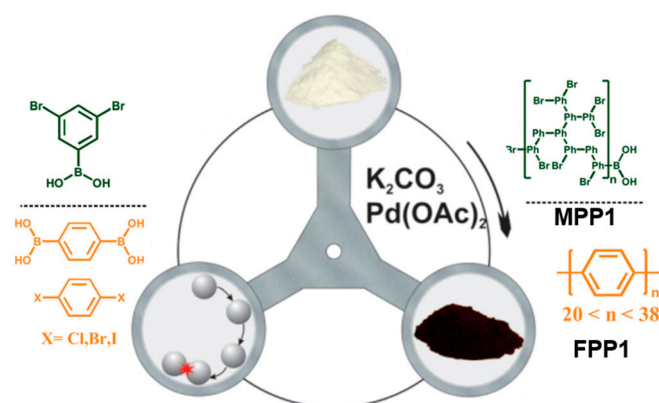


Figure 10. Mechanochemical synthesis of polyphenylenes and hyperbranched derivatives. Reproduced with the permission of reference [85].

In addition to linear polymers, by using 3,5-dibromophenylboronic acid, the same approach was used to prepare a microporous hyperbranched polymer (MHP1) with a high temperature resistance and high yields in short reaction times.

Among the FPPs, polyfluorenes (PFs) [86] and their copolymers [87–89] exhibited advanced optoelectronic properties due to the influence of micro- and macrostructural organization in a solid-state and/or polymer film [90–97]. Therefore, the method of preparation of PFs can strongly influence their properties and performance.

Very recently, Nelson's group developed [98] a mechanochemical Suzuki polymerization method to prepare polyfluorene-conjugated polymers, such as poly(9,9-di-*n*-octylfluorenyl-2,7-diyl) (PF), poly(9,9-dioctylfluorene-alt-benzothiadiazole) (PFBT), and poly[(9,9-bis(3'-(*N,N*-dimethylamino)propyl)-2,7-fluorene)-alt-2,7-(9,9-dioctylfluorene)] (PFN) (Figure 11). The authors provided extended research on optimizing the reaction conditions such as the milling frequency and time and catalyst loading on the polymer molecular weights, dispersity, and yield. It was found that the Pd catalyst loading played a key role, while the milling time and frequency played a less important role.

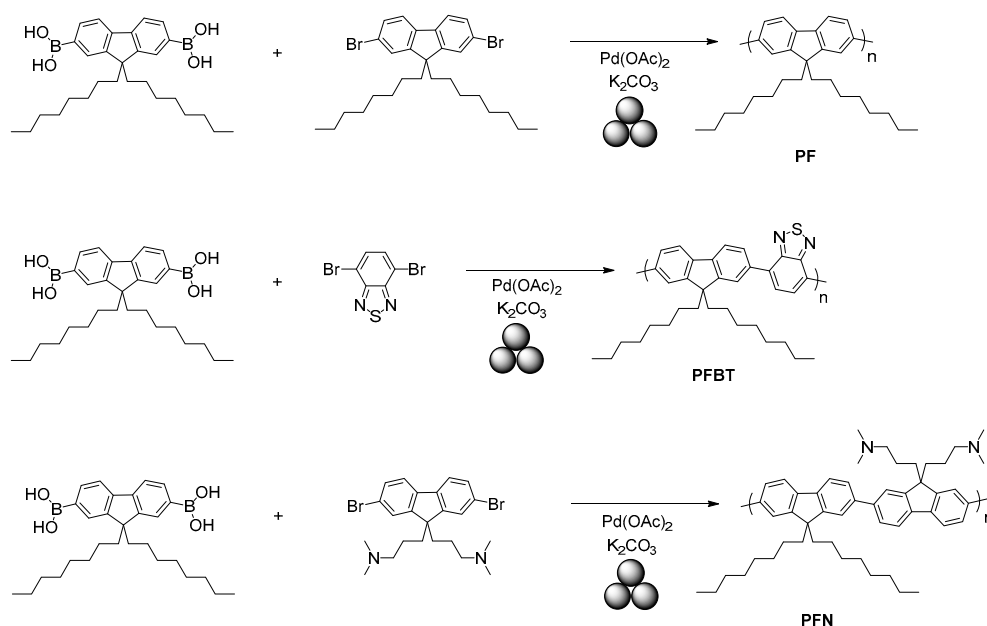


Figure 11. Mechanochemical synthesis of polyfluorenes.

Moreover, a polyelectrolyte, PFN-Br, was developed using solvent-assisted ball-milling polymerization from a PFN polymer during mechanochemical quaternization at the ter-

minal amino groups. This material could have a potential application as an electron-interface-layer material in OFETs, OLEDs, OPVs, and perovskite solar cells to improve the interfacial properties.

2.6. Mechano-synthesis of Polyanylines and Polyamines

Polyanilines (PANIs) are the most famous conductive polymers [99–101] due to the simplicity of their preparation via connecting the 1,4-coupling of aniline monomer parts, environmental stability, ability to be doped by protonic acids, and, finally, ability to exist in different oxidation states, such as (a) leucoemeraldine, (b) emeraldine (salt/base), and (c) pernigraniline. PANIs and their derivatives/co-polymers are extensively applied in rechargeable batteries, photovoltaic cells, gas separation membranes, chemical sensors, anti-corrosion coatings, microwave absorption electromagnetic interference shielding, electrodes and supercapacitors, reagents for photothermal therapy, etc. [102–104].

Zhou and co-authors reported a PANI synthesis method by using the interaction of aniline sulphate with ammonium persulphate in a pan mill (600 rpm) and, for comparison, by means of mortar grinding for 40 min [105]. The authors observed that for two pan mill cycles, the molecular weight of PANI was lower than for the mortar-grinded mixture, whilst it was almost equal after ten cycles, and twice as large after twenty cycles.

In 2011, a PANI mechano-synthesis method was reported [106] by mixing anilinium hydrochloride with different oxidants (ammonium persulphate, FeCl_3 , and AgNO_3) with a mortar (5 min) with the following treatment of the obtained powder with air. According to the authors, the PANI formed with ammonium persulphate in 24 h, while after one week with FeCl_3 and AgNO_3 , only short oligomers and branched non-conductive polymers were obtained using Fe^{3+} or Ag^+ .

Posudievsky and co-authors reported the synthesis of highly conductive PANI (22.3 S/cm) by means of grinding anilinium chloride and ammonium persulphate in a planetary mill by using an agate jar and milling balls at 300 rpm [107]. For comparison, the PANI was obtained via a solvent-based procedure. Even though the molecular weights of both polymers were comparable, a better conductivity was observed for the PANI obtained by using methano-synthesis. This difference was attributed by the authors to the influence of mechanical stress on the polymer during its mechanochemical preparation, and an increased conductivity of the PANI obtained via the solvent-based procedure by post-synthesis mechanochemical treatment was observed.

It worth mentioning that, earlier, Huang and coauthors [108] reported a PANI synthesis method using the interaction between anilinium chloride and ammonium persulfate in a stainless-steel jar using stainless-steel milling balls (5–10 mm) at 600 rpm in a Pulverizette 7 planetary micromill for 1 h. Highly conductive PANI was obtained in a 65% yield at an ammonium persulfate:ammonium chloride ratio = 1:2. A conductivity of 0.01 S/cm was observed.

Bhandari and Khastgir reported the mechano-synthesis of ultra-long nanofibrous PANI by means of grinding anilinium chloride and ammonium peroxydisulphate in the presence and absence of citric acid (as a dopant) by using a mortar and pestle for 30 min [109]. According to the authors, citric acid influenced the morphology of the PANI via hydrogen bonding and provided the doping of PANI, while in the absence of citric acid, the PANI was “undoped”. In addition, this in situ doping dramatically influenced the electrochemical behavior of the PANI.

In 2021, a mechanochemical oxidative polymerization method using an OMe derivative of PANI, poly(*o*-anisidine) (POA), and POA-protected silver nanoparticles, POA@Ag, was reported [110] (Figure 12). As a first step, the authors subjected anisidinium sulphate (OA-HSO_4) to mechanopolymerization as a monomer to produce POA in the presence of ammonium persulphate as an oxidant. In the second step, POA was formed in situ in the presence of AgNO_3 as both an oxidant and a metal precursor to produce POA-protected silver nanoparticles, POA@Ag. In this case, an equimolar amount of OA-HSO_4 and AgNO_3 (2 mM, 0.34 g) were hand-ground in mortar with a pestle for 10 min, resulting in the

formation of a slurry, which in 15–45 min converted into a pale green color, with the final product being the green-colored emeraldine salt. Ag nanoparticles were also immobilized in the obtained polymer matrix. Based on electrochemical studies, the interconversion of POA between the leucoemeraldine \leftrightarrow emeraldine and emeraldine \leftrightarrow pernigraniline redox transformation and the redox responses of the AgNPs was observed. The authors suggested the potential application of **POA@Ag** as an electrocatalyst. In addition, the electrochemical response of **POA@Ag** toward dopamine via cyclic voltammetry (CV), differential pulse voltammetry (DPV), and chronoamperometry was observed with the electrochemical stability of **POA@Ag** for the dopamine determination being in the 10–130 μM range and with a limit of detection (LOD) as low as 2.8 μM . In a chronoamperometry-based method, dopamine was detected in the range of 5–45 μM (0.83 μM LOD). Finally, a **POA@Ag**/GCE-modified electrode for the determination of dopamine from mixtures was prepared, which was able to operate at a 160 mV potential difference with repeatability after 15 and 30 days of immersion.

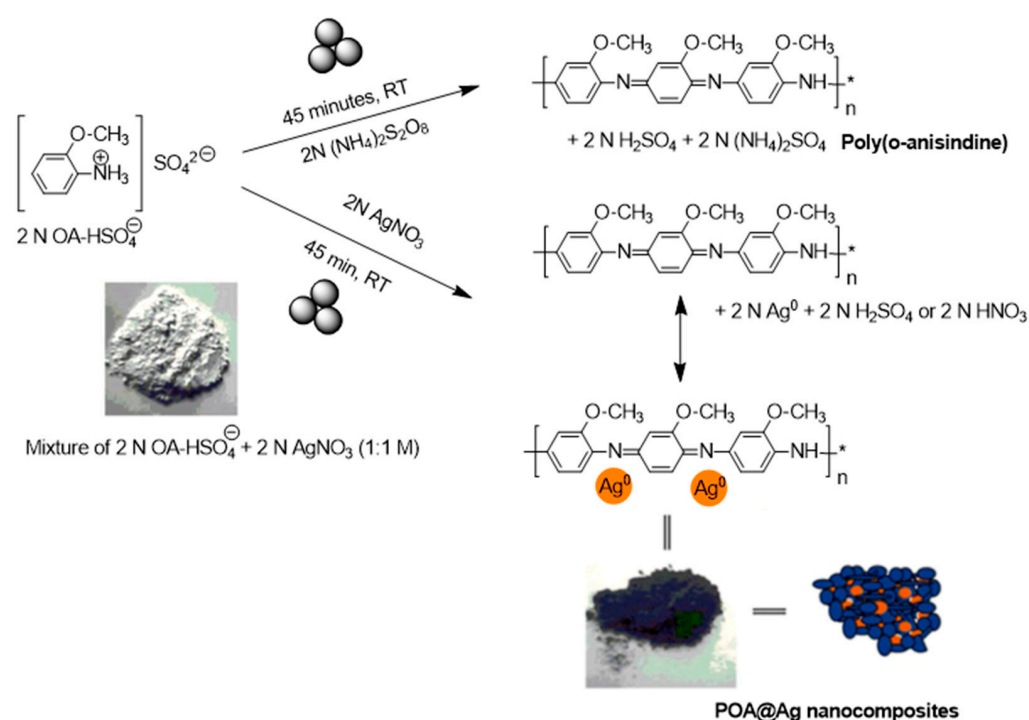


Figure 12. Mechanosynthesis of POA and POA@Ag, “*” represents a multiplication sign. Reproduced with the permission of reference [110].

It worth mentioning that mechanochemical approaches are widely used for the preparation of PANI-based nanocomposites via the in situ formation of PANI upon ball-milling or grinding anilines and oxidants (if needed) with different additives, such as porous clays, carbon nanotubes, metal, and oxide nanoparticles, etc. [111].

Very recently, Yang, He, and co-authors reported [112] (Figure 13) an efficient method for the construction of graphene/PANI composites via a one-pot high-energy ball-milling process. In this process, aniline molecules acted as both the intercalator for the exfoliation of graphite and the monomer for mechanochemical polymerization into PANI clusters on the in situ exfoliated graphene sheets. The obtained graphene/PANI composite electrode delivered a large specific capacitance of 886 F·g⁻¹ at 5 mV·s⁻¹ with a high retention of 73.4% at 100 mV·s⁻¹. In addition, a high energy density of 40.9 W·h·kg⁻¹ was achieved by the graphene/polyaniline-based symmetric supercapacitor at a power density of 0.25 kW·kg⁻¹, and the supercapacitor also maintained 89.1% of the initial capacitance over 10,000 cycles.

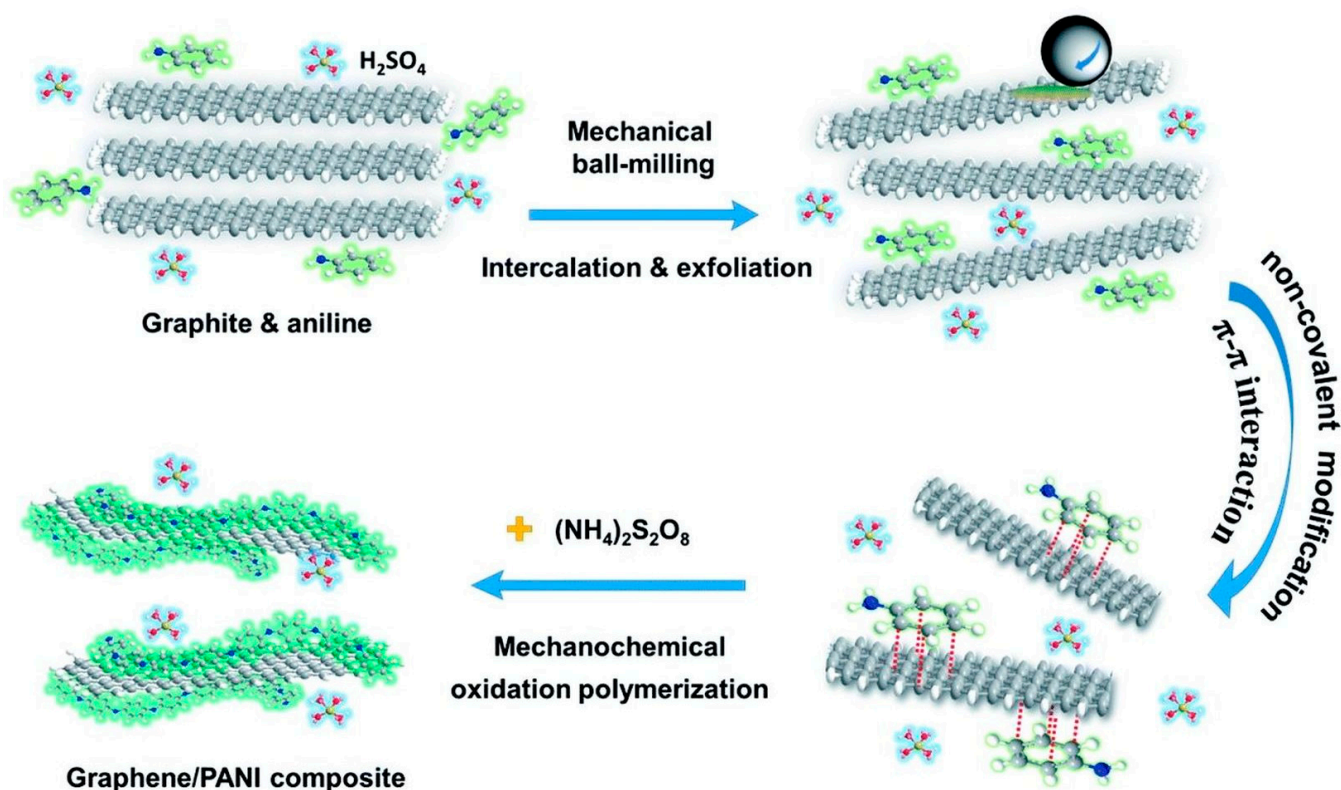


Figure 13. Mechanosynthesis of graphene/PANI composites. Reproduced with the permission of reference [112].

Along with PANIs, anilines can be involved in the preparation of other polyamines by using mechanosynthesis. For example, Lou and co-authors reported [113] (Figure 14) a mechanosynthesis method of highly crosslinked *N*-connected polymers by using solvent-free and mechanochemical conditions (NUT-71-F) and, for comparison, a conventional solvent-based approach (NUT-71-S). According to the authors, upon mechanical grinding in a mortar, NUT-71-F exhibited a higher reaction yield in comparison with NUT-71-S (70.8% vs. 49.8%) due to the greater crosslinking degree and different linkage ways.

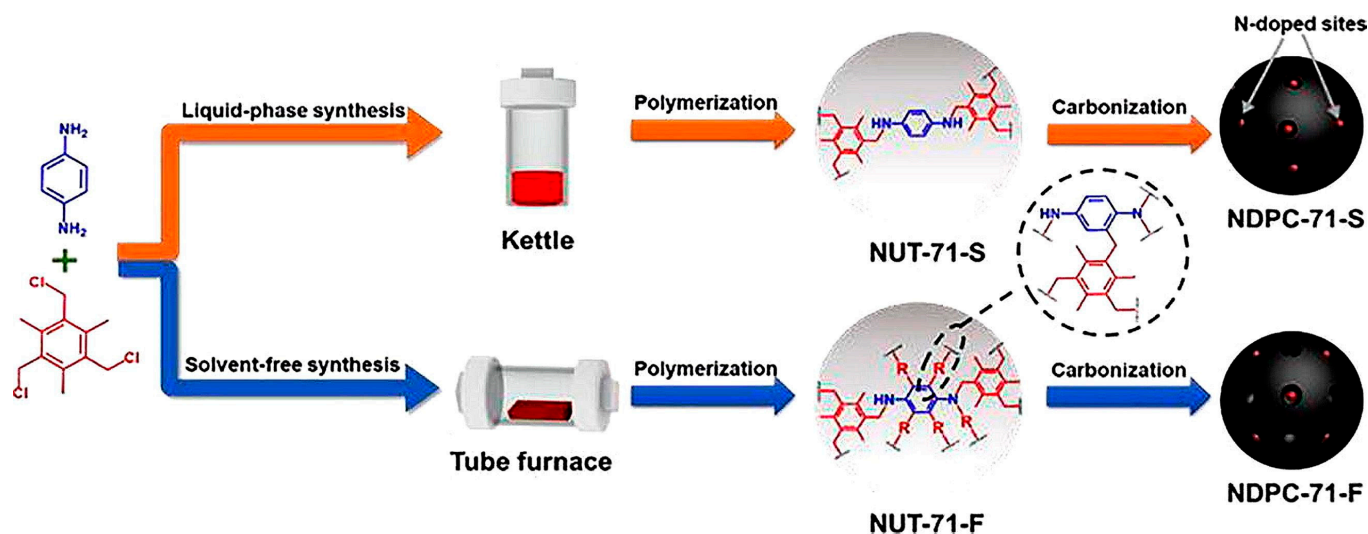


Figure 14. Mechanosynthesis of *N*-connected polymers. Reproduced with the permission of reference [113].

In addition, by the carbonization of both polymers at different temperatures (500 °C, 600 °C, 700 °C, and 800 °C, respectively), the authors constructed N-doped porous carbons (NDPCs) and evaluated their affinity and selectivity for a gaseous N₂/CO₂ (85/15, v/v) mixture. It was found that **NDPC-71-F** (from mechanochemically prepared **NUT-71-F**) possessed a higher specific surface area and a larger pore volume compared to **NDPC-71-S** (obtained from **NUT-71-S**) and could separate CO₂ from a N₂/CO₂ mixture more efficiently. For instance, the pore size varied from 0.52 to 0.70 nm in **NDPC-71-F-700**, while it only varied from 0.43 to 0.51 nm in **NDPC-71-S-700**. It should be noted that increasing the carbonization temperature to 800 °C excessively enlarged the pore size, making them unable to effectively capture CO₂.

Moreover, no significant reduction in the CO₂ adsorption capacity of **NDPC-71-F-700** was detected after six regeneration experiments, which is crucial for potential practical application.

2.7. Mechano-synthesis of Organic Porous Polymers

Organic porous polymers (OPPs) have several unique features, such as high surface/contact surface area, highly rigid permanent porous structure, low skeletal density along with good chemical and thermodynamic stability, and, thus, porous polymers have a wide range of applications [114,115], including catalytic applications [116–120], gas storage [121–125], and gas separation [126,127]. The most convenient approach to creating OPPs is the so-called bottom-up building concept, which involves the stepwise building of the desired material by using monomer units containing various functionalities by using either TM-catalyzed transformations, such as cross-coupling reactions [128], Friedel–Crafts alkylations [129], and cyclotrimerization reactions [130], or TM-free approaches, such as Schiff base formation reactions [131], amidisation reactions [132], etc. In these approaches, in order to achieve permanent micro- and mesoporosity, an initial intensive mixing is crucial. In addition, shrinkage of the obtained material upon the drying step takes place after the removal of the absorbed organic vapors or liquids. Finally, the low solubility of most OPPs remains the main challenge, and in some cases the solution-based procedures may suffer from the precipitation of reagents/products to produce OPPs with a low degree of polymerization [133].

The ball-milling polymerization process allows the obtaining of polymeric porous materials without solvents, has wide applicability, has an easy synthetic set-up (ball-milling jar), is low-cost, has a simple pre- and post-treatment, and has little or no influence and dependence on the environment. Therefore, ball-milling-assisted polymerization may be considered to be a versatile tool for the synthesis of OPPs.

For instance, Grätz, Borchardt, and coauthors [134] reported a mechanochemical synthesis method of producing hyper-crosslinked polymers (**HCP**), which may be considered as some of the most promising OPP candidates [135], by using a solvent-free Friedel–Crafts alkylation reaction involving 4,4'-bis(chloromethyl)-1,1'-biphenyl (Figure 15). In a typical procedure, 4,4'-bis(chloromethyl)-1,1'-biphenyl and FeCl₃ were milled in a zirconium oxide milling vessel filled with 22 zirconium oxide balls (10 mm) in a Fritsch Pulverisette 7 mill at 500 rpm for 35 min to produce a porous polymer with BET surface areas of up to 1720 m²·g⁻¹ and pore volumes of up to 1.55 cm³·g⁻¹ with a narrower pore size distribution compared to their solvent-based analogues. The obtained polymer exhibited a preferable adsorption of benzene vapors over cyclohexane, which was, according to the authors, due to the strong π–π interactions with the aromatic framework.

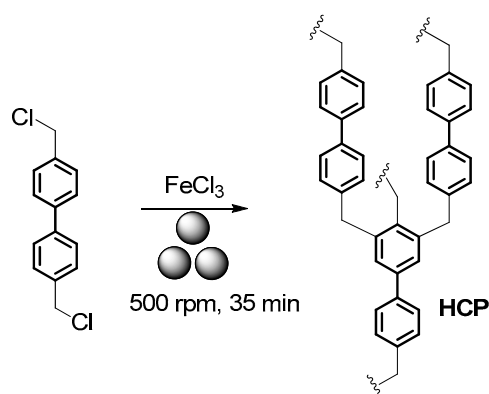


Figure 15. Mechanochemical synthesis of HCP.

Later, the same group reported [136] a more advanced mechanochemical synthesis method of producing a microporous thiophene polymer (MTP) via oxidative polymerization in the presence of NaCl as a bulking material (Figure 16). In a typical procedure, 1,3,5-tris(2-thienyl)benzene, FeCl_3 , and the inert bulking material NaCl (to control the abrasion [137]) were mixed in a stainless-steel grinding jar with 22 grinding balls (10 mm) at 400 rpm in a Fritsch Pulverisette 7 premium line planetary ball mill for 60 min. In the optimization studies, the ball size (10–15 mm) and milling speed (400–600 rpm) were optimized for the highest yields (up to 98%). The obtained MTP exhibited a specific surface area of $1850 \text{ m}^2 \cdot \text{g}^{-1}$ and a pore volume of $0.95 \text{ cm}^3 \cdot \text{g}^{-1}$ with a narrow pore size distribution and with one major pore at 1.6 nm. According to the authors, the observed surface area was almost twice as high as the reported values for the solution-based process. The obtained material absorbed Ar and N_2 , and the authors did not observe the typical swelling behavior, which was most probably due to the higher degree of polymerization and crosslinking and therefore the more rigid structure of the polymer.

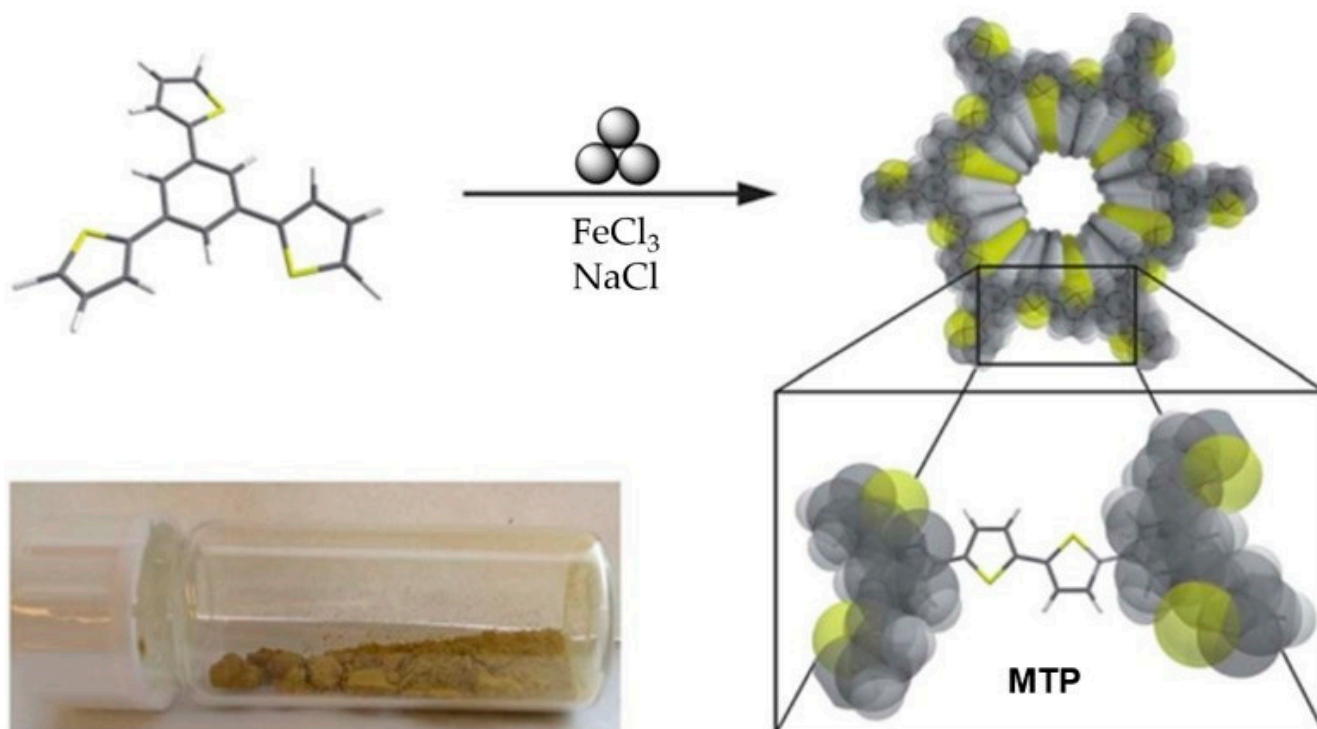


Figure 16. Mechanochemical synthesis of MTP. Reproduced with the permission of reference [136].

In addition, to prove the generality of the developed strategy of mechanochemistry of polymers, the authors applied our procedure to the synthesis of previously synthesized polycarbazoles [138] via FeCl_3 -catalyzed polymerization in a vibrational ball mill (Retsch mixer-mill 400 at 30 Hz for 0.5 h) to produce a microporous carbazol-based polymer starting from 1,3,5-tri(9-carbazolyl)-benzene as a promising candidate for CO_2 storage. The polycarbazole obtained by using the above-mentioned advanced protocol exhibited a surface area of $1710 \text{ m}^2 \cdot \text{g}^{-1}$, which exceeded the previously reported [139] values by a factor of two.

Very recently, the same group reported the mechanochemistry of another microporous polymer (**MPP1-2**) [140] by using a Friedel–Crafts alkylation of 1,3,5-triphenylbenzene with two organochloride cross-linking agents, dichloromethane (DCM) (**MPP1**) and chloroform (CHCl_3) (**MPP2**), respectively (Figure 17). In a typical protocol, TPB and DCM or CHCl_3 in the presence of AlCl_3 were milled in a zirconium oxide milling jar with 22 milling balls (10 mm) for 1 h at 30 Hz to produce the target polymers. DCM-linked polymers were found to be flexible and extremely sensitive towards parameter changes, which even enabled the synthesis of a polymer with a BET surface area of $1670 \text{ m}^2 \cdot \text{g}^{-1}$, while the CHCl_3 -linked polymers were more rigid with a high porosity (the surface area was found to be $1280 \text{ m}^2 \cdot \text{g}^{-1}$). Based on green metrics calculations, the mechanochemistry had an advantage over the solvent-based one in terms of the reaction time (0.5 h vs. 48 h), mass intensity (4 vs. 31–37), mass productivity (23 vs. 3), and overall E-factor (1.8–2 vs. 30–36).

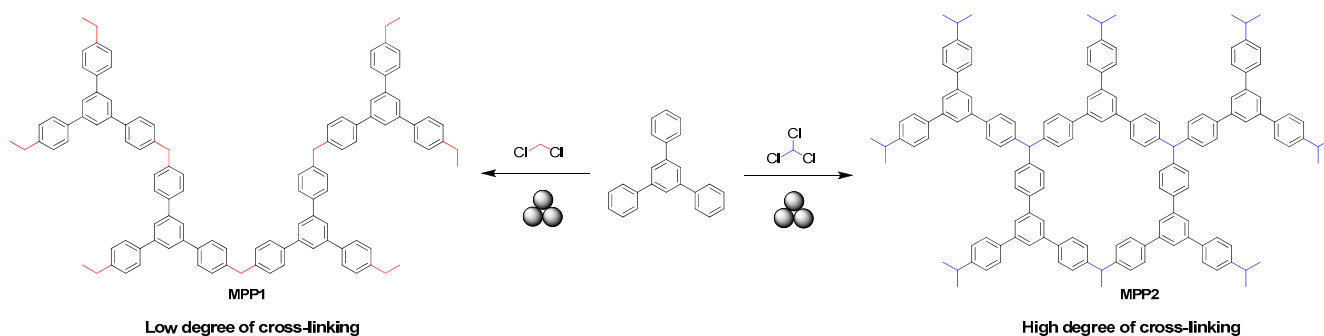


Figure 17. Mechanochemistry of DCM- and CHCl_3 -linked OPPs (**MPP1-2**).

Ladder-like polymers of intrinsic microporosity (PIMs) with contorted sites have been reported as a family of soluble porous polymers and have been successfully utilized in membrane-based gas separations [141,142]. In these polymers, ladder-like monomer units are the main contributor for achieving the high porosity of the resulting polymers. Thus, Tian, Liu, Jin, Dai, and coauthors [143] reported a solvent-free mechanochemistry method of producing a novel family of soluble fluorescent nanoporous polymer networks based on 3,3,3',3'-tetramethyl-2,2',3,3'-tetrahydro-1,1'-pibio[indene]-6,6'-diol (**BPSPI-OH**). The authors used either a solvent-mediated FeCl_3 -initiated oxidative coupling reaction (A) or mechanochemical approach (B) (Figure 18). As a result, three polymers, **OCP-NPN1-3**, were obtained.

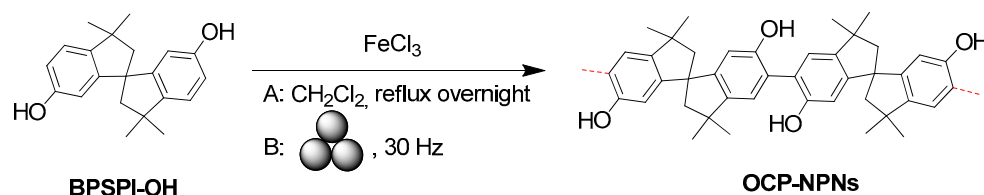


Figure 18. Synthesis of OCP-NPN1-3.

According to the authors, for the polymer **OCP-NPN-1**, prepared under ball-milling conditions in the presence of FeCl_3 , the Brunauer–Emmett–Teller (BET) surface area was lower

than that of the polymer prepared via the solvent-mediated method (470 vs. $834 \text{ m}^2 \cdot \text{g}^{-1}$). Moreover, dissolving and re-precipitating the polymer from CH_2Cl_2 resulted in a decrease in the BET surface area (205 vs. $470 \text{ m}^2 \cdot \text{g}^{-1}$) due to the possible swelling of **MC-OCP-NPN-1**. However, the BET value could be increased to $319 \text{ m}^2 \cdot \text{g}^{-1}$ by means of the repeated dissolution and re-precipitating process in $\text{CH}_2\text{Cl}_2:\text{EtOH} = 1:4$. For the ball-milling approach, the FeCl_3 content was critical, and by increasing the FeCl_3 amount to 4 mol. eq. the authors obtained **OCP-NPN-3** with a BET surface area of $733 \text{ m}^2 \cdot \text{g}^{-1}$. In experiments with gas absorption, the **MC-OCP-NPN-1** sample showed selectivity to CO_2 over CH_4 ($20.9 \text{ cm}^3 \cdot \text{g}^{-1}$ vs. $5.8 \text{ cm}^3 \cdot \text{g}^{-1}$ of uptake). Finally, a **MC-OCP-NPN-1** mixed-matrix membrane was prepared, and this matrix membrane exhibited an efficient CO_2/CH_4 separation with a high CO_2 permeability of 675 and a CO_2/CH_4 selectivity of 25.

Covalent 1,3,5-triazine-based frameworks are another promising scaffold for constructing porous polymers with surface areas $>3200 \text{ m}^2/\text{g}$ [144] combined with high chemical and thermal stability up to $700 \text{ }^\circ\text{C}$ [145,146], and they are commonly prepared via nitrile cyclotrimerization approaches [147–149]. 1,3,5-Triazine-based porous polymers have a wide range of applications, such as electrode materials in supercapacitors [150] or lithium-sulfur batteries [151–153], materials for CO_2 capture [154–156], etc. Another approach to such polymers involves an AlCl_3 -mediated Friedel–Crafts alkylation method by using cyanuric chloride as a core unit [154]. Lübken and Borchardt recently reported a mechanochemical approach to producing *s*-triazine-based porous polymers (**TPPs**) [157] by using an *s*-triazine node (cyanuric chloride) and various aromatic coupling partners upon ball-milling in the presence of stoichiometric amounts of AlCl_3 as an activating reagent and ZnCl_2 as a bulking agent (Figure 19).

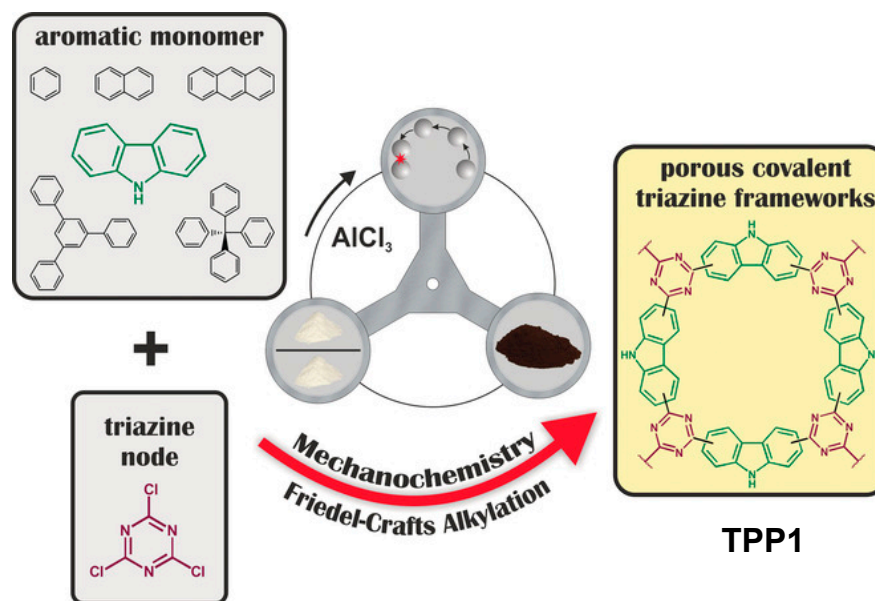


Figure 19. Mechanochemical synthesis of **TPPs**, “*” means collision event between the milling balls. Reproduced with the permission of reference [157].

In a typical procedure, cyanuric chloride, AlCl_3 , and ZnCl_2 were reacted in either a tungsten carbide grinding jar with 22 balls (10 mm) or in a zircon oxide grinding jar with 22 tungsten carbide balls (10 mm) in a Fritsch Pulverisette 7 planetary ball mill at 800 rpm. In model experiments using carbazole, the authors observed a 32 % yield of polymer **TPP1** after 15 min and a 98% yield after 60 min, and the porosity of the material remained constant from this point on ($740 \text{ m}^2 \cdot \text{g}^{-1}$ due to N_2 physisorption). According to a BET model, the specific surface area for **TPP1** was $570 \text{ m}^2 \cdot \text{g}^{-1}$, and a sharp pore size distribution was observed, showing two micropores of 0.5 nm and 1.0 nm, respectively. By using optimized reaction conditions, the authors obtained other polymers by using benzene

(**TPP2**, specific surface area of $170 \text{ m}^2 \cdot \text{g}^{-1}$, 0.20 nm pore size, 5% yield), naphthalene (**TPP3**, specific surface area of $110 \text{ m}^2 \cdot \text{g}^{-1}$, 0.17 nm pore size, 2% yield), and tetraphenylmethane (**TPP4**, specific surface area of $390 \text{ m}^2 \cdot \text{g}^{-1}$, 0.43 nm pore size, 3% yield).

A carbazole-based OPP (**CzPP**) with a high surface area and excellent stability was reported as a promising porous material to capture and separate CO_2 under mild conditions [158] (Figure 20). To achieve this tetrakis(4-(9H-carbazol-9-yl)phenyl)methane and FeCl_3 were reacted in an agate tube with ball milling for 2 h to produce **CzPP** in a 91% yield. As calculated by DFT, the median pore width for C was 0.75 nm, and the total pore volume was $0.63 \text{ cm}^3/\text{g}$. As for gas sorption, **CzPP** demonstrated selectivity toward CO_2 over N_2 in a binary gas mixture.

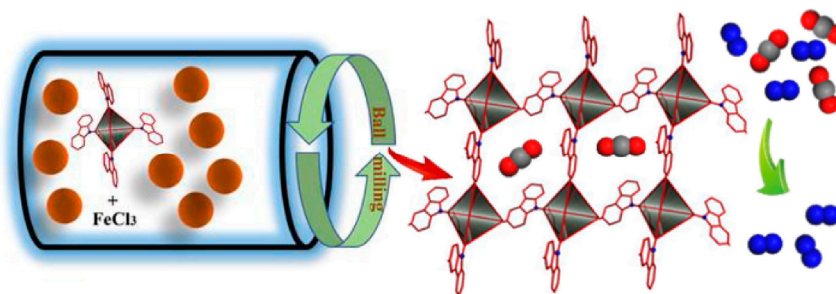


Figure 20. Mechanochemistry of **CzPP**. Reproduced with the permission of reference [158].

Another type mechanochemically prepared **CzPP** was reported by Wang and co-authors [159] (Figure 21). In addition to carbazole, a fullerene moiety was introduced into the polymer structure. In a typical case, di-(9H-carbazol-9-yl) methylene fullerenes, **Ful-Cz-1** and **Ful-Cz-2**, were reacted together with FeCl_3 in a stainless-steel jar with stainless-steel balls in a Retsch mixer-mill 400 at 30 Hz for 30 min to produce the polymer **FulCP** in an 82% yield. The solution method required 12 h with a tedious purification method. The amount of FeCl_3 had a great influence on the specific surface area of the products prepared by the solvent method, but it did not affect the specific surface area of products prepared by the ball-milling method. The pore size distribution of the mechanochemically prepared **FulCP** was mainly 0.64 nm, which implied a microporous nature, and the dominant pore size distribution peaks for the **FulCP** prepared by the solution-based method were at 0.54 and 1.18 nm. The Brunauer–Emmett–Teller specific surface area of the **FulCP** prepared by the ball-milling method ($1015 \text{ m}^2 \cdot \text{g}^{-1}$) was higher than that produced by traditional solvent method ($920 \text{ m}^2 \cdot \text{g}^{-1}$). The obtained polymer was further used to prepare a **FulCP**-supported palladium complex (**FulCP-Pd**) as a heterogeneous catalyst in a deallylation reaction. The conversion efficiency of **FulCP-Pd** with different substrates ranged from 76% to 92%, and the conversion of allyl phenyl ether was the highest (92%). Based on all the above, an obvious positive influence of both the presence of a fullerene moiety in the monomer structure and the mechanochemistry on the increased porosity of the **FulCP** and the effectiveness of **FulCP-Pd** was demonstrated.

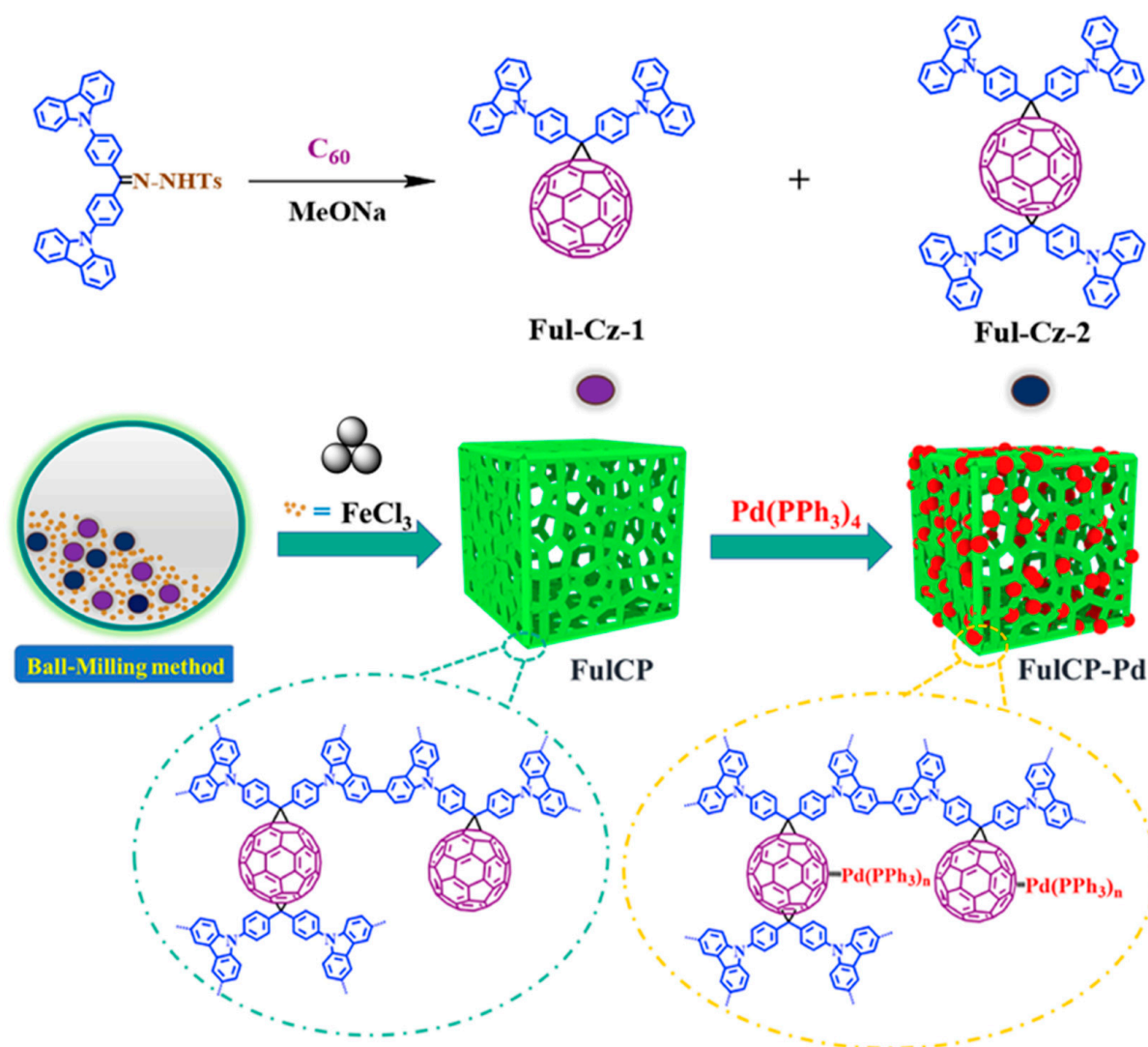


Figure 21. Mechanochemical synthesis of FulCP. Reproduced with the permission of reference [159].

It is worth mentioning that fullerene polymers have a wide range of applications for organic electronics, photovoltaics, and (photo)catalysis [160], including catalytic applications [161], energy storage and transfer [162], and photovoltaics [163].

Pan and coworkers reported a dopamine-sensing system based on a mechanochemically synthesized tetraphenylethylene-based porous polymer (TPEPP) [164] (Figure 22). In the first step, the authors obtained a tetraphenylethylene (TPE)-based porous organic polymer by means of the reaction of catalytic amounts of $FeCl_3$, 1,3,5-triformylbenzene, and 1,1,2,2-tetraphenylethene in a zirconium oxide milling vessel with zirconium oxide milling balls in a planetary mill at 500 rpm for 35 min to produce the target TPEPP. After that, the obtained TPEPP was carbonized, and a carbon quantum dot (CQD) was prepared. In the last step, a CQD/chitosan-graphene composite film electrode was constructed for the electrochemiluminescence-based determination of dopamine. The thus constructed electrode presented good repeatability and a high sensitivity to dopamine with a wide linear range from 0.06 to 1.6 μM . In addition, a satisfactory detection limit of 0.028 μM ($S/N = 3$) was achieved. Finally, the authors demonstrated the possibility of detecting the dopamine concentration in human fluids (namely in serum samples).

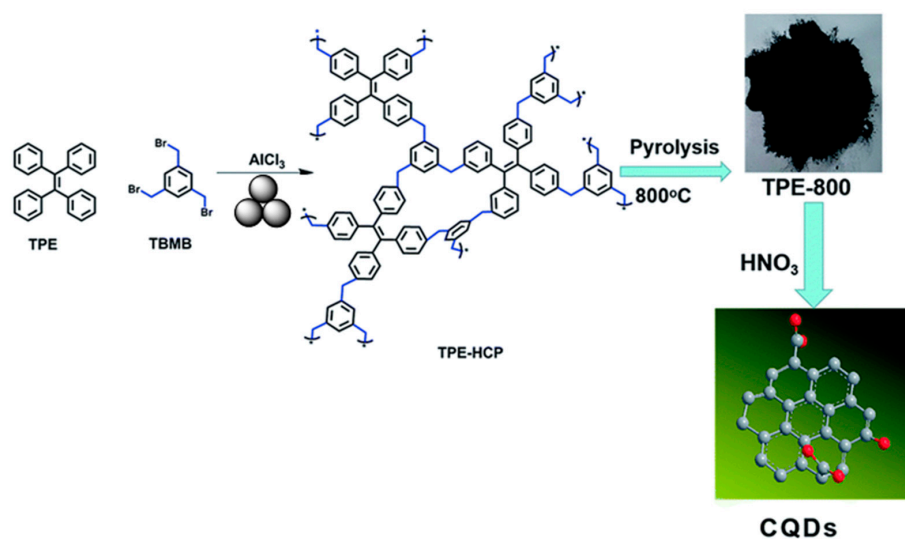


Figure 22. Mechanochemical synthesis of TPEPP. Reproduced with the permission of reference [164].

2.8. Mechanochemical Post-Modification of Polymers

Mechanochemical methods are readily used for polymer post-modification and for the preparation of co-polymers. Below, some of the most representative examples are highlighted.

Ohura and co-authors reported [165] (Figure 23) the synthesis of diblock copolymers of microcrystalline cellulose (MCC) and poly 2-hydroxyethyl methacrylate (pHEMA) produced by mechanochemical polymerization under vacuum and at room temperature. The tacticities of the HEMA sequences in the MCC-block-pHEMA varied according to the reaction time, namely the fraction of pHEMA in the MCC-block-pHEMA increased up to 21 mol% with increasing the fracture time (~6 h). According to the authors, cellulose acted as a radical polymerization initiator that was capable of controlling the stereoregularity. During the mechanochemical synthesis, the mechanical fracturing of the polymer produced free-radical chain-ends, and their recombination resulted in block copolymers.

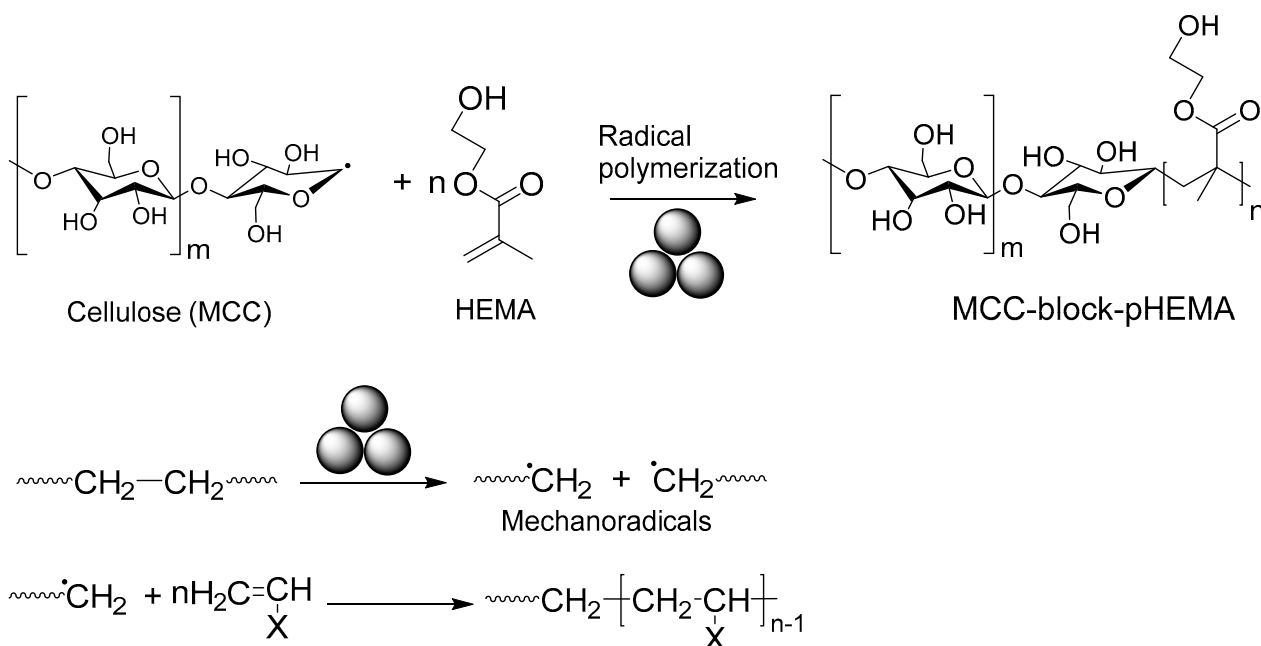


Figure 23. Mechanochemical synthesis of MCC-block-pHEMA.

Ohn and Kim reported [166] (Figure 24) the mechanochemical post-modification of poly(styrene-co-4-vinylbenzaldehyde) via solid-state Schiff's base formations with a series of amines and amine derivatives. In a typical case, polymer, amine, and ammonium carbamate salt were reacted in a stainless-steel jar with three stainless-steel balls (7 mm) at 30 Hz for 30 min. Regardless of the nature of the amine, a 98–99% conversion with a PDI of 1.16–1.33 was observed.

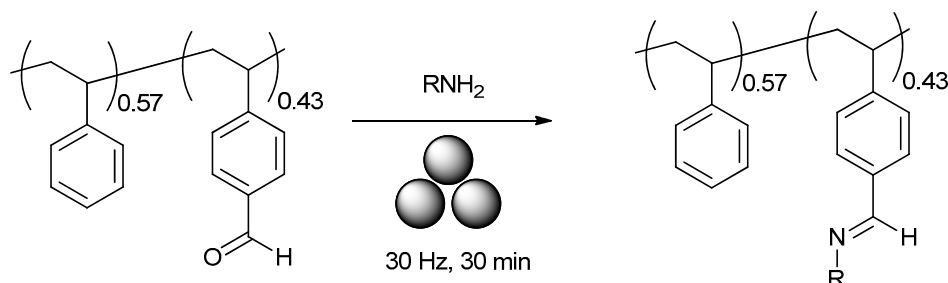


Figure 24. Mechanochemical post-modification of poly(styrene-co-4-vinylbenzaldehyde).

In addition to poly(styrene-co-4-vinylbenzaldehyde), the mechanochemical post-modification of poly(4-vinylbenzaldehyde) (Figure 25) was carried out.

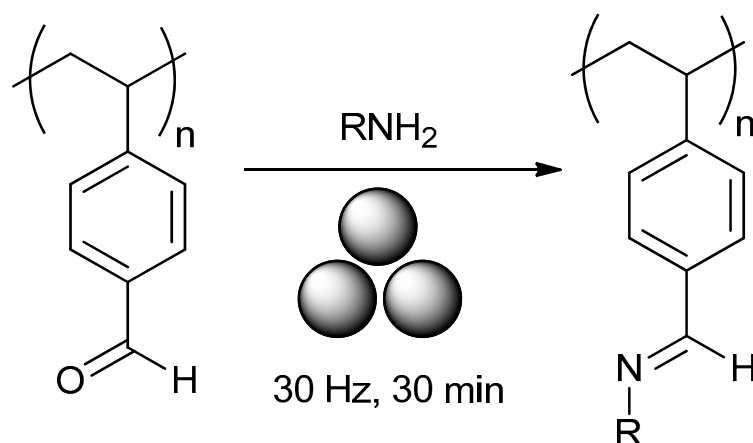


Figure 25. Mechanochemical post-modification of poly(4-vinylbenzaldehyde).

In a similar way, Kim and coauthors [167] developed a mechanochemical approach for the post-modification of diblock copolyethers PEEGE-b-PAHGE obtained from monomers of ethoxyethyl glycidyl ether (EEGE) and azidohexyl glycidyl ether (AHGE) (Figure 26). The mechanochemical modification of the polymer-appended amino-functionality with a highly hydrophobic and potent anticancer agent, cinnamaldehyde, through an imine linkage. The resulting polymer–drug conjugates were further self-assembled into polymeric micelles, which was confirmed by dynamic light scattering and atomic force microscopy. In the obtained Schiff's base-appended polymers, **IM1-4**, the *pH*-responsive cleavage of the imine linkages under acidic conditions led to the release of cinnamaldehyde with a concomitant disassembly of the polymeric micelles.

Frišćić and co-authors reported a solid-state mechanochemical ω -functionalization of poly(ethylene glycol) (PEG) with tosyl (Figure 27a), bromide (Figure 27b), thiol (Figure 27c), carboxylic acid (Figure 27d), and amine (Figure 27e) functionalities (Figure 27) in good-to-quantitative yields [168]. In the most typical case, a PEG polymer and the corresponding reagents were milled in a Teflon jar with one 10 mm Zr ball in a Retsch Mixer Mill 400 at 30 Hz for 15–90 min to produce the desired polymer. Depending on a nature of PEG, its molecular weights, and the type of functionality introduced, the reaction was completed in 15–90 min and provided the desired polymers in 42–99% yields (according to ^1H NMR).

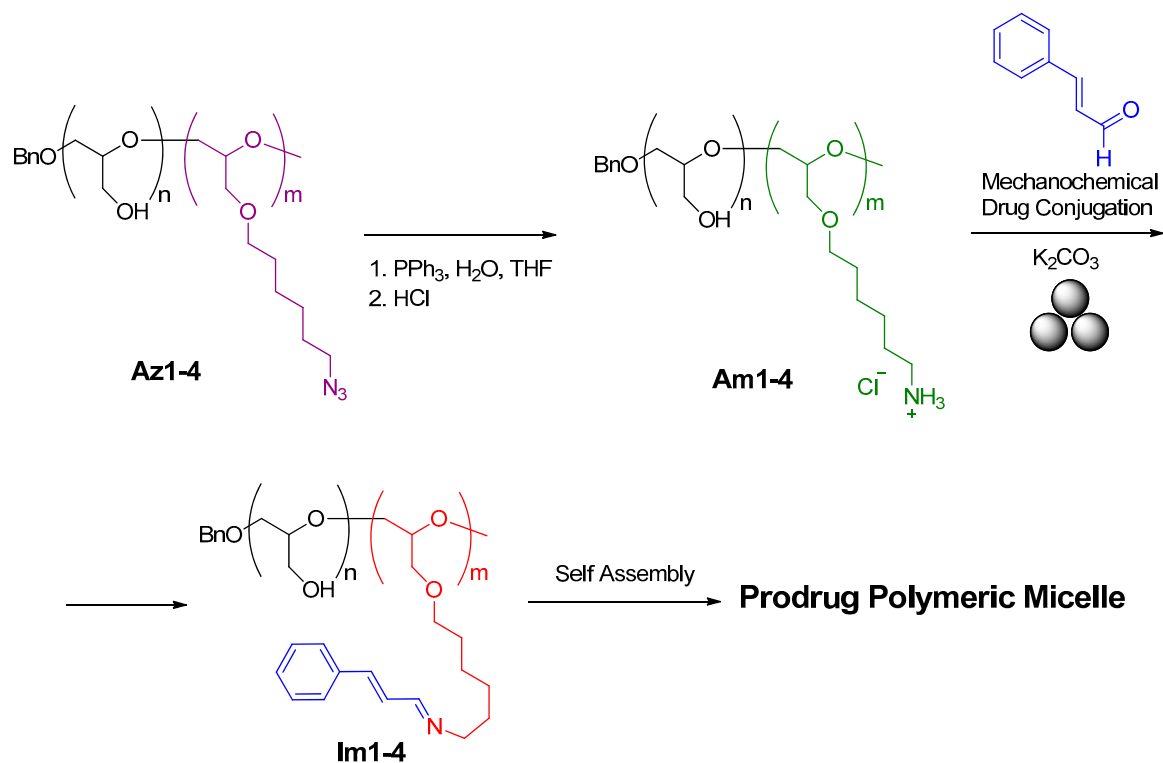


Figure 26. Mechanochemical post-modification of AM1-4.

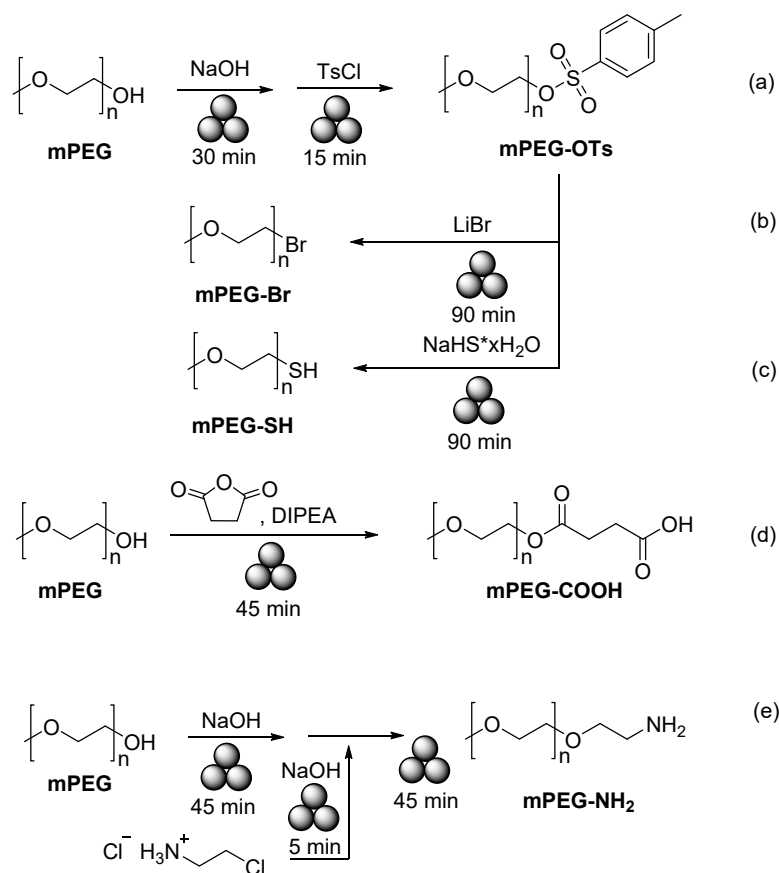


Figure 27. Mechanochemical ω -functionalization of PEG, tosyl (a), bromide (b), thiol (c), carboxylic acid (d), and amine (e).

Ashlin and Hobbs reported [169] a mechanochemical post modification of polymers **BrP1-4** with thiol moieties (Figure 28). In a typical case, the polymer and the corresponding thiol were milled in a stainless-steel grinding jar equipped with three stainless-steel grinding balls (7 mm) using a Retsch MM-400 ball mill at 30 Hz for 15 min to produce the thiol-containing polymers in up to a 95% yield. To prove the concept, the authors prepared a chloromethyl-functionalized-polymer by the co-polymerisation of styrene and 4-vinylbenzyl chloride, and, under similar conditions, the substitution of the chlorine atom of the benzyl chloride moiety with various thiols was also achieved in high yields.

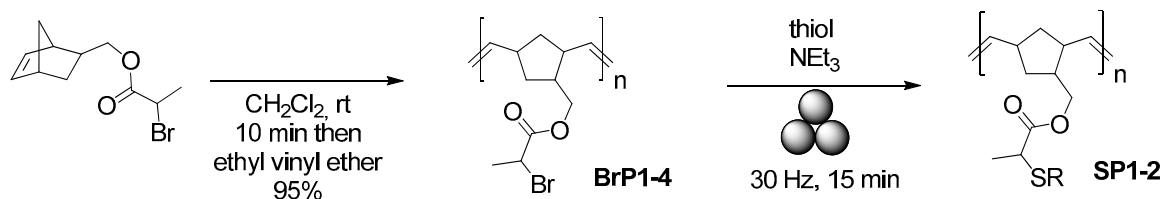


Figure 28. Mechanochemical post-modification with thiols.

It worth mentioning that similar types of parent polymers could be obtained using ruthenium-alkylidene catalysts for ring-closing and cross-metathesis reactions under ball-milling conditions [170,171].

A quite rare example of the post-modification/co-polymerization of two polymers via host–guest interaction under mechanochemical conditions was reported by Park and co-authors [172] (Figure 29). In the first step, the authors prepared two polymers bearing cyclodextrin (**P-Ac β CD(x)**) (Figure 29a) and adamantane (**P-Ad(y)**) (Figure 29b) moieties. In the second step, by mixing the host and guest polymers by planetary ball milling, the supramolecular host–guest-based polymer was obtained. According to the authors, the toughness of the supramolecular materials prepared by ball milling (way e) was approximately two-to-five times higher than that of supramolecular materials prepared by casting as a conventional method (way Figure 29c) or kneading (way Figure 29d), and during repeated ball-milling treatments, the obtained supramolecular polymers were able to maintain their mechanical properties. These materials are readily applicable as self-healable bulk materials and coatings, as their fractured pieces can be re-adhered within 10 min.

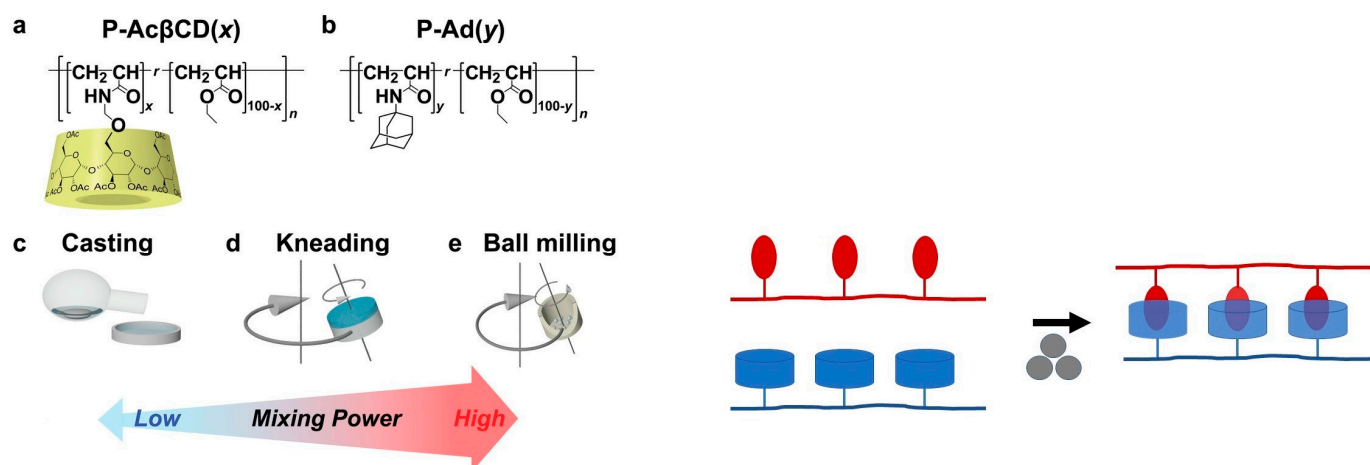


Figure 29. Mechanochemical post-modification via host–guest interactions, cyclodextrin (**P-Ac β CD(x)**) moieties (a), adamantane (**P-Ad(y)**) moieties (b), ball milling (e), conventional method (c) and kneading (d). Reproduced with the permission of reference [172].

3. Conclusions and Future Perspectives

In summary, mechanochemical synthesis has become a convenient tool for the construction of functional homo- or co-polymers of various types, as well as for the fast and efficient introduction of extra functionalities into terminal ends as well as side arms with a high degree of conversion of previously prepared polymers without rupturing the main polymer backbone. The main advantages of mechanosynthesis over the conventional solvent-based synthesis of functional polymers include the much shorter reaction times (from several minutes to several hours), the absence of the influence of the solvent (and its associated solubility problems for both the target polymer and starting monomers), the lower mass intensity, the higher mass productivity, and, finally, the much lower overall E-factors (due to absence of solvents). The most-accepted mechanism of mechanopolymerization involves the formation of short-lived mechanoradicals generated by mechanical force, which was confirmed in some publications by using radical traps, such as TEMPO [173]. Due to strong influence of the mechanical force in the reaction, the hardness and size/weight of the milling balls, as well as intensity of the ball-milling, are critical for achieving a high monomer conversion, and the best results were reported for tungsten carbide (WC) and zirconium oxide (ZrO) and for agate milling balls (pests) and with a milling speed/frequency higher than 300 rpm/5 Hz. The avoidance of solvents is beneficial for the mechanosynthesis of various organic porous polymers, which are hardly available by means of conventional solvent-based methods with a high porosity/surface area for gas separation or catalysis. Finally, mechanochemical synthesis is a convenient tool for the preparation of functional polymers by using industrial by-products, for instance, sulfur [174,175], industrial/post-consumer wastes [6,176], or agricultural wastes [177].

For polymer characterization, a set of common methods is usually used. The most important factor is the molecular weight of the functional polymer. Most often, gel permeation chromatography (GPC) [19,41,73] and size-exclusion chromatography (SEC) [40,42] are used for the estimation of molecular weights. The main limitation of GPC/SEC is the solubility of the analyzed polymer in organic solvents (most commonly DMF and THF). More rarely, MALDI-TOF analysis [51] or, if it is possible to end-cap the obtained polymer with ^1H NMR- or IR-distinguishable end-groups, NMR- [54] or IR-based [178] end-group analysis are used. Additionally, ^1H NMR analysis can be used for the estimation of monomer(s) conversion [40]. During mechanosynthesis, the heating of the milling balls and, as a result, the local overheating of the reaction media/obtained polymer is questioned in the literature [179]. Therefore, the thermal degradation of polymers, i.e., the maximum temperature at which a polymer can be manufactured and processed, is another important parameter and can be used for polymer analysis. To estimate the thermal stability of polymers, thermogravimetric analysis (TGA) for measuring polymer weight changes as a function of temperature and time, differential thermal analysis (DTA) for measuring the glass and other polymer transitions, or differential scanning calorimetry (DSC) for investigating the response of polymers to heating, such as the melting of a crystalline polymer or the glass transition, can be used. For porous functional polymers such as those used for catalytic applications and gas separation/storage, the contact surface area and pore (voids) size is important. To estimate these values, the Brunauer–Emmett–Teller (BET) surface area can be calculated for the theoretical estimation of the physical adsorption of gas molecules (most commonly N_2) on a solid surface of the polymer [135,140,143,157].

Regarding future perspectives, one can mention the following. Among the TM-catalyzed mechanochemical approaches to producing functional polymers, Pd-catalyzed processes, which have been widely explored for small molecules [180], have so far only been reported by a few cases of Suzuki cross-coupling reactions [52,84,85,98]. So, in the near future, one might expect the interest in mechanopolymerization reactions based on the Buchwald, Stille, or Sonogashira cross-coupling protocols to grow.

Finally, in terms of closed-loop economic systems, to solve the end-of-use problem for synthetic polymers, one needs to either design polymers composed of a certain type of dynamic bonds that are capable of effective bonding and reversible cleaving and/or

to develop of efficient ways for the polymers to depolymerize into monomers. For the first approach, to break the dynamic bonds, high temperatures are usually required and, in some cases, the thermo-degradation of polymers may occur, which may influence their mechanical properties [181,182]. We mentioned [71] one example above of the mechanosynthesis of diketoenamine-bond-connected polymers for ready mechanopolymerization/depolymerization at room temperature. Very recently, another type of room-temperature-recyclable polymer containing dynamic maleic acid tertiary amide bonds was reported [183].

For commercial polymers, their thermal degradation, except their monomers, produces multiple decomposition products, including oligomers and char [184–188]. In addition, ball-milling-assisted depolymerization might be a greener alternative to the above-mentioned approaches, which was recently suggested in reports on the mechanochemistry-assisted depolymerization of polyethylene terephthalate (PET) [189] and polystyrene [190].

Author Contributions: Conceptualization, G.V.Z. and B.C.R.; methodology, W.K.A.A.-I., I.L.N., V.A.P., G.V.Z., D.S.K., I.S.K., S.S. and A.F.K.; investigation, W.K.A.A.-I., G.V.Z., I.L.N., V.A.P., D.S.K., I.S.K., S.S. and A.F.K.; data curation, W.K.A.A.-I., I.L.N., D.S.K., I.S.K., S.S. and A.F.K.; writing—original draft preparation, G.V.Z., W.K.A.A.-I., I.L.N., D.S.K., I.S.K., S.S., A.F.K. and B.C.R.; writing—review and editing, G.V.Z., W.K.A.A.-I., I.L.N., D.S.K., I.S.K., S.S., A.F.K. and B.C.R.; supervision, G.V.Z. and B.C.R.; project administration, G.V.Z. and B.C.R.; funding acquisition, G.V.Z. and B.C.R. All authors have read and agreed to the published version of the manuscript.

Funding: This research was funded by the Council for Grants of the President of the Russian Federation, Grant # NSh-1223.2022.1.3 (for the Section 2.3), Ministry of Science and Higher Education of the Russian Federation, Reference # 075-15-2022-1118, dated 29 June 2022 (all other sections).

Institutional Review Board Statement: Not applicable.

Data Availability Statement: The data presented in this study are available on request from the corresponding author.

Acknowledgments: The study was done with a support of the state assignment of IOS UB RAS (Theme No. AAAA-A19-119011790132-7).

Conflicts of Interest: The authors declare no conflict of interest.

References

1. Cintas, P.; Tabasso, S.; Veselov, V.V.; Cravotto, G. Alternative reaction conditions: Enabling technologies in solvent-free protocols. *Curr. Opin. Green Sustain. Chem.* **2020**, *21*, 44–49. [[CrossRef](#)]
2. Mottillo, C.; Frišćić, T. Advances in Solid-State Transformations of Coordination Bonds: From the Ball Mill to the Aging Chamber. *Molecules* **2017**, *22*, 144. [[CrossRef](#)] [[PubMed](#)]
3. Krusenbaum, A.; Grätz, S.; Tigineh, G.T.; Borchardt, L.; Kim, J.G. The mechanochemical synthesis of polymers. *Chem. Soc. Rev.* **2022**, *51*, 2873–2905. [[CrossRef](#)] [[PubMed](#)]
4. Cuccu, F.; De Luca, L.; Delogu, F.; Colacino, E.; Solin, N.; Mocci, R.; Porcheddu, A. Mechanochemistry: New Tools to Navigate the Uncharted Territory of “Impossible” Reactions. *ChemSusChem* **2022**, *15*, e202200362. [[CrossRef](#)] [[PubMed](#)]
5. Zhang, Z.-Y.; Zhang, F.-S.; Yao, T.Q. An environmentally friendly ball milling process for recovery of valuable metals from e-waste scraps. *Waste Manag.* **2017**, *68*, 490–497. [[CrossRef](#)]
6. Capuano, R.; Bonadies, I.; Castaldo, R.; Cocca, M.; Gentile, G.; Protopapa, A.; Avolio, R.; Errico, M.E. Valorization and Mechanical Recycling of Heterogeneous Post-Consumer Polymer Waste through a Mechano-Chemical Process. *Polymers* **2021**, *13*, 2783. [[CrossRef](#)]
7. Bento, O.; Luttringer, F.; El Dine, T.M.; Pétry, N.; Bantreil, X.; Lamaty, F. Sustainable Mechanochemistry of Biologically Active Molecules. *Eur. J. Org. Chem.* **2022**, *2022*, e202101516. [[CrossRef](#)]
8. Ying, P.; Yu, J.; Su, W. Liquid-assisted grinding mechanochemistry in the synthesis of pharmaceuticals. *Adv. Synth. Catal.* **2021**, *363*, 1246–1271. [[CrossRef](#)]
9. Pedrazzo, A.R.; Cecone, C.; Trotta, F.; Zanetti, M. Mechanochemistry of β -cyclodextrin polymers based on natural deep eutectic solvents. *ACS Sustain. Chem. Eng.* **2021**, *9*, 14881–14889. [[CrossRef](#)]
10. Xuan, M.; Schumacher, C.; Bolm, C.; Göstl, R.; Herrmann, A. The mechanochemical synthesis and activation of carbon-rich π -conjugated materials. *Adv. Sci.* **2022**, *9*, 2105497. [[CrossRef](#)]
11. Frišćić, T.; Mottillo, C.; Titi, H.M. Mechanochemistry for Synthesis. *Angew. Chem. Int. Ed.* **2020**, *59*, 1018–1029. [[CrossRef](#)]

12. Chiang, C.K.; Drury, M.A.; Gau, S.C.; Heeger, A.J.; Louis, E.J.; MacDiarmid, A.G.; Park, Y.W.; Shirakawa, H. Synthesis of Highly Conducting Films of Derivatives of Polyacetylene, (CH)_x. *J. Am. Chem. Soc.* **1978**, *100*, 1013–1015. [[CrossRef](#)]
13. Basescu, N.; Liu, Z.-X.; Moses, D.; Heeger, A.J.; Naarmann, H.; Theophilou, N. High electrical conductivity in doped polyacetylene. *Nature* **1987**, *327*, 403–405. [[CrossRef](#)]
14. Foyle, L.D.P.; Hicks, G.E.J.; Pollit, A.A.; Seferos, D.S. Polyacetylene Revisited: A Computational Study of the Molecular Engineering of N-type Polyacetylene. *J. Phys. Chem. Lett.* **2021**, *12*, 7745–7751. [[CrossRef](#)]
15. Hernangómez-Pérez, D.; Gunasekaran, S.; Venkataraman, L.; Evers, F. Solitonics with polyacetylenes. *Nano Lett.* **2020**, *20*, 2615–2619. [[CrossRef](#)]
16. Bustamantea, C.M.; Scherlis, D.A. Doping and coupling strength in molecular conductors: Polyacetylene as a case study. *Phys. Chem. Chem. Phys.* **2021**, *23*, 26974–26980. [[CrossRef](#)]
17. Banerjee, J.; Dutta, K. A short overview on the synthesis, properties and major applications of poly(p-phenylene vinylene). *Chem. Pap.* **2021**, *75*, 5139–5151. [[CrossRef](#)]
18. Burroughes, J.H.; Bradley, D.D.C.; Brown, A.R.; Marks, R.N.; Mackay, K.; Friend, R.H.; Burns, P.L.; Holmes, A.B. Light-emitting diodes based on conjugated polymers. *Nature* **1990**, *347*, 539–541. [[CrossRef](#)]
19. Ravnsbæk, J.B.; Swager, T.M. Mechanochemical Synthesis of Poly(Phenylene Vinylenes). *ACS Macro. Lett.* **2014**, *3*, 305–309. [[CrossRef](#)]
20. Wang, L.-X.; Li, X.-G.; Yang, Y.-L. Preparation, properties and applications of polypyrroles. *React. Funct. Polym.* **2001**, *47*, 125–139. [[CrossRef](#)]
21. Grgur, B.N.; Gvozdenovi, M.M.; Stevanovi, J.; Jugović, B.Z.; Marinović, V.M. Polypyrrole as possible electrode materials for the aqueous-based rechargeable zinc batteries. *Electrochim. Acta* **2008**, *53*, 4627–4632. [[CrossRef](#)]
22. Wang, G.; Qu, Q.; Wang, B.; Shi, Y.; Tian, S.; Wu, Y. An Aqueous Electrochemical Energy Storage System Based on Doping and Intercalation: Ppy//LiMn₂O₄. *ChemPhysChem* **2008**, *9*, 2299–2301. [[CrossRef](#)] [[PubMed](#)]
23. Carquignya, S.; Sanchez, J.-B.; Berger, F.; Lakard, B.; Lallemand, F. Ammonia gas sensor based on electrosynthesized polypyrrole films. *Talanta* **2009**, *78*, 199–206. [[CrossRef](#)] [[PubMed](#)]
24. Kim, J.H.; Lau, K.T.; Shepherd, R.; Wu, Y.; Wallace, G.; Diamond, D. Performance characteristics of a polypyrrole modified polydimethylsiloxane (PDMS) membrane based microfluidic pump. *Sens. Actuators A* **2008**, *148*, 239–244. [[CrossRef](#)]
25. Cui, S.; Mao, J.; Rouabhia, M.; Elkoun, S.; Zhang, Z. A biocompatible polypyrrole membrane for biomedical applications. *RSC Adv.* **2021**, *11*, 16996–17006. [[CrossRef](#)]
26. Sun, J.; Wang, G.; Zhang, H.; Zhang, B.; Hu, C. Facile fabrication of a conductive polypyrrole membrane for anti-fouling enhancement by electrical repulsion and in situ oxidation. *Chemosphere* **2021**, *270*, 129416. [[CrossRef](#)]
27. Pang, A.L.; Arsad, A.; Ahmadipour, M. Synthesis and factor affecting on the conductivity of polypyrrole: A short review. *Polym. Adv. Technol.* **2021**, *32*, 1428–1454. [[CrossRef](#)]
28. Carrasco, P.M.; Grande, H.J.; Cortazar, M.; Alberdi, J.M.; Areizaga, J.; Pomposo, J.A. Structure–conductivity relationships in chemical polypyrroles of low, medium and high conductivity. *Synth. Met.* **2006**, *156*, 420–425. [[CrossRef](#)]
29. Blinova, N.V.; Stejskal, J.; Trchová, M.; Prokeš, J.; Omastová, M. Polyaniline and polypyrrole: A comparative study of the preparation. *Eur. Polym. J.* **2007**, *43*, 2331–2341. [[CrossRef](#)]
30. Posudievsky, O.Y.; Goncharuk, O.A.; Pokhodenko, V.D. Mechanochemical preparation of conducting polymers and oligomers. *Synth. Met.* **2010**, *160*, 47–51. [[CrossRef](#)]
31. Posudievsky, O.Y.; Kozarenkoa, O.A. Effect of monomer/oxidant mole ratio on polymerization mechanism, conductivity and spectral characteristics of mechanochemically prepared polypyrrole. *Polym. Chem.* **2011**, *2*, 216–220. [[CrossRef](#)]
32. Ueno, N.; Sugita, K.; Seki, K.; Inokuchi, H. Electron Affinities of polystyrene and poly(2-vinylpyridine) by low-energy electron inelastic scattering. *Jpn. J. Appl. Phys.* **1985**, *24*, 1156. [[CrossRef](#)]
33. Semerak, S.N.; Frank, C.W. Energy migration in the aromatic vinyl polymers. 5. Poly(2-vinyl naphthalene) and polystyrene. *Can. J. Chem.* **1985**, *63*, 1328–1332. [[CrossRef](#)]
34. Frank, C.W.; Harrah, L.A. Excimer formation in vinyl polymers. II. Rigid solutions of poly(2-vinylnaphthalene) and polystyrene. *J. Chem. Phys.* **1974**, *61*, 1526. [[CrossRef](#)]
35. Masayuki, A.; Takeshi, T.; Hiroaki, B.; Masahiro, I.; Koichiro, H. Intramolecular Dimer and Excimer Phosphorescence of Poly(2-vinylnaphthalene) and Copolymers of 2-Vinylnaphthalene and Phenyl Vinyl Ketone. *Bull. Chem. Soc. Jpn.* **1978**, *51*, 3643–3644.
36. Nakamura, H.; Kitamura, H.; Shinji, O.; Saito, K.; Shirakawa, Y.; Takahashi, S. Development of polystyrene-based scintillation materials and its mechanisms. *Appl. Phys. Lett.* **2012**, *101*, 261110. [[CrossRef](#)]
37. Sen, I.; Penumadu, D.; Williamson, M.; Miller, L.F.; Green, A.D.; Mabe, A.N. Thermal neutron scintillator detectors based on poly(2-vinylnaphthalene) composite films. *IEEE Trans. Nucl. Sci.* **2011**, *58*, 1386–1393. [[CrossRef](#)]
38. Berns, S.; Boyarintsev, A.; Hugon, S.; Kose, U.; Sgalaberna, D.; De Roeck, A.; Lebedynskiy, A.; Sibilievad, T.; Zhmurin, P. A novel polystyrene-based scintillator production process involving additive manufacturing. *JINST* **2020**, *15*, P10019. [[CrossRef](#)]
39. Kapłan, Ł.; Moskal, G. Blue-emitting polystyrene scintillators for plastic scintillation dosimetry. *Bio-Algorithms Med-Syst.* **2021**, *17*, 191–197. [[CrossRef](#)]
40. Cho, H.Y.; Bielawski, C.W. Atom transfer radical polymerization in the solid-state. *Angew. Chem.* **2020**, *132*, 14033–14039. [[CrossRef](#)]

41. Hasegawa, M.; Kimata, M.; Takahashi, I. Mechanochemical polymerization of styrene initiated by the grinding of layered clay minerals. *Adv. Powder Technol.* **2007**, *18*, 541–554. [[CrossRef](#)]
42. Yoo, K.; Lee, G.S.; Lee, H.W.; Kim, B.-S.; Kim, J.G. Mechanochemical solid-state vinyl polymerization with anionic initiator. *Faraday Discuss.* **2023**, *241*, 413–424. [[CrossRef](#)] [[PubMed](#)]
43. Kim, H.C.; Kim, J.S.; Kim, K.S.; Park, H.K.; Baek, S.; Ree, M. Synthesis and characterization of new, soluble polyazomethines bearing fluorene and carbazole units in the backbone and solubility-improving moieties in the side group. *J. Polym. Sci. A* **2004**, *42*, 825–834. [[CrossRef](#)]
44. Iwan, A.; Boharewicz, B.; Parafiniuk, K.; Tazbir, I.; Gorecki, L.; Sikora, A.; Filapek, M.; Schab-Balcerzak, E. New air-stable aromatic polyazomethines with triphenylamine or phenylenevinylene moieties towards photovoltaic application. *Synth. Met.* **2014**, *195*, 341–349. [[CrossRef](#)]
45. Wojtkiewicz, J.; Iwan, A.; Pilch, M.; Boharewicz, B.; Wójcik, K.; Tazbir, I.; Kaminska, M. Towards designing polymers for photovoltaic applications: A DFT and experimental study of polyazomethines with various chemical structures. *Spectrochim. Acta A* **2017**, *181*, 208–217. [[CrossRef](#)]
46. Bolduc, A.; Al Ouahabi, A.; Mallet, C.; Skene, W.G. Insight into the isoelectronic character of azomethines and vinylenes using representative models: A spectroscopic and electrochemical study. *J. Org. Chem.* **2013**, *78*, 9258–9269. [[CrossRef](#)]
47. Şenol, D.; Kolcu, F.; Kaya, İ. Synthesis, characterization, electrical conductivity and fluorescence properties of polyimine bearing phenylacetylene units. *J. Fluoresc.* **2016**, *26*, 1579–1590. [[CrossRef](#)]
48. Yen, H.J.; Liou, G.S. Recent advances in triphenylamine-based electrochromic derivatives and polymers. *Polym. Chem.* **2018**, *9*, 3001–3018. [[CrossRef](#)]
49. Kaya, I.; Kilavuz, E.; Temizkan, K. Synthesis, characterization and quantum yields of multichromic poly(azomethine)s containing carbazole unit. *Arab. J. Chem.* **2020**, *13*, 1335. [[CrossRef](#)]
50. Lei, T.; Guan, M.; Liu, J.; Lin, H.-C.; Pfattner, R.; Shaw, L.; McGuire, A.F.; Huang, T.-C.; Shao, L.; Cheng, K.-T.; et al. Biocompatible and totally disintegrable semiconducting polymer for ultrathin and ultralight weight transient electronics. *Proc. Natl. Acad. Sci. USA* **2017**, *114*, 5107–5112. [[CrossRef](#)]
51. Grätz, S.; Borchardt, L. Mechanochemical polymerization—Controlling a polycondensation reaction between a diamine and a dialdehyde in a ball mill. *RSC Adv.* **2016**, *6*, 64799. [[CrossRef](#)]
52. Al-Ithawi, W.K.A.; Khasanov, A.F.; Valieva, M.I.; Baklykov, A.V.; Chistiakov, K.A.; Ladin, E.D.; Kovalev, I.S.; Nikonov, I.L.; Kim, G.A.; Platonov, V.A.; et al. (Mechano)synthesis of azomethine- and terpyridine-linked diketopyrrolopyrrole-based polymers. *Chim. Techno. Acta.* **2023**, *10*, 202310204. [[CrossRef](#)]
53. Bao, W.W.; Li, R.; Dai, Z.C.; Tang, J.; Shi, X.; Geng, J.T.; Deng, Z.F.; Hua, J. Diketopyrrolopyrrole (DPP)-Based Materials and Its Applications: A Review. *Front. Chem.* **2020**, *8*, 679. [[CrossRef](#)]
54. Al-Ithawi, W.K.A.; Platonov, V.A.; Kovalev, I.S.; Kopchuk, D.S.; Nikonov, I.L.; Zyryanov, G.V.; Ranu, B.C. Mechano-synthesis of aza-linked dibenzo[*a,c*]phenazine-containing polymers. *Bull. Commun. B* **2023**, *5*, 8.
55. Helms, B.A.; Russell, T.P. Polymer chemistries enabling cradle-to-cradle life cycles for plastics. *Chem* **2016**, *1*, 813–819. [[CrossRef](#)]
56. Rahimi, A.R.; García, J.M. Chemical recycling of waste plastics for new materials production. *Nat. Rev. Chem.* **2017**, *1*, 0046. [[CrossRef](#)]
57. García, J.M.; Robertson, M.L. The future of plastics recycling. *Science* **2017**, *358*, 870–872. [[CrossRef](#)]
58. Hong, M.; Chen, E.Y.-X. Chemically recyclable polymers: A circular economy approach to sustainability. *Green Chem.* **2017**, *19*, 3692–3706. [[CrossRef](#)]
59. MacArthur, E. Beyond plastic waste. *Science* **2017**, *358*, 843. [[CrossRef](#)]
60. Schneiderman, D.K.; Hillmyer, M.A. 50th Anniversary perspective: There is a great future in sustainable polymers. *Macromolecules* **2017**, *50*, 3733–3749. [[CrossRef](#)]
61. La Manria, F.P. Closed loop recycling: A case study of films for greenhouse. *Polym. Degrad. Stab.* **2010**, *95*, 285–288. [[CrossRef](#)]
62. Min, H. Analysis for strategy of closed-loop supply chain with dual-recycling channel. *Int. J. Prod. Econ.* **2013**, *144*, 510–520.
63. Bruno, L. Emergy assessment of benefits of closed-loop recycling accounting for material losses. *Ecol. Model.* **2015**, *315*, 77–87.
64. Denissen, W.; Rivero, G.; Nicolaÿ, R.; Leibler, L.; Winne, J.M.; Du Prez, F.E. Vinylogous urethane vitrimers. *Adv. Funct. Mater.* **2015**, *25*, 2451–2457. [[CrossRef](#)]
65. Fortman, D.J.; Brutman, J.P.; Cramer, C.J.; Hillmyer, M.A.; Dichtel, W.R. Mechanically activated, catalyst-free polyhydroxyurethane vitrimers. *J. Am. Chem. Soc.* **2015**, *137*, 14019–14022. [[CrossRef](#)]
66. Obadia, M.M.; Mudraboyina, B.P.; Serghei, A.; Montarnal, D.; Drockenmuller, E. Reprocessing and recycling of highly cross-linked ion-conduction networks through trans-alkylation exchanges of C–N bonds. *J. Am. Chem. Soc.* **2015**, *137*, 6078–6083. [[CrossRef](#)]
67. Taynton, P.; Ni, H.; Zhu, C.; Yu, K.; Loob, S.; Jin, Y.; Qi, H.J.; Zhang, W. Repairable woven carbon-fiber composites with full recyclability enabled by malleable polyimine networks. *Adv. Mater.* **2016**, *28*, 2904–2909. [[CrossRef](#)]
68. Yu, K.; Shi, Q.; Dunn, M.L.; Wang, T.; Qi, H.J. Carbon fiber reinforced thermoset composite with near 100% recyclability. *Adv. Funct. Mater.* **2016**, *26*, 6098–6106. [[CrossRef](#)]
69. Röttger, M.; Domenech, T.; Van Der Weegen, R.; Breuillac, A.; Nicolaÿ, R.; Leibler, L. High-performance vitrimers from commodity thermoplastics through dioxaborolane metathesis. *Science* **2017**, *356*, 62–65. [[CrossRef](#)]
70. Snyder, R.L.; Fortman, D.J.; De Hoe, G.X.; Hillmyer, M.A.; Dichtel, W.R. Reprocessable acid-degradable polycarbonate vitrimers. *Macromolecules* **2018**, *51*, 389–397. [[CrossRef](#)]

71. Christensen, P.R.; Scheuermann, A.M.; Loeffler, K.E.; Helms, B.A. Closed-loop recycling of plastics enabled by dynamic covalent diketoenamine bonds. *Nat. Chem.* **2019**, *11*, 442–448. [[CrossRef](#)]
72. Nagarajan, V.; Mohanty, A.K.; Misra, M. Perspective on polylactic acid (pla) based sustainable materials for durable applications: Focus on toughness and heat resistance. *ACS Sustain. Chem. Eng.* **2016**, *4*, 2899–2916. [[CrossRef](#)]
73. Lee, G.S.; Moon, B.R.; Jeong, H.; Shin, J.; Kim, J.G. Mechanochemical synthesis of poly(lactic acid) block copolymers: Overcoming the miscibility of the macroinitiator, monomer and catalyst under solvent-free conditions. *Polym. Chem.* **2019**, *10*, 539–545. [[CrossRef](#)]
74. Werpy, T.; Petersen, G. *Top Value Added Chemicals from Biomass, Volume I—Results of Screening for Potential Candidates from Sugars and Synthesis Gas*; Pacific Northwest National Laboratory, US Department of Energy: Richland, WA, USA, 2004.
75. Marshall, A.; Jiang, B.; Gauvin, R.M.; Thomas, C.M. 2,5-Furandicarboxylic Acid: An intriguing precursor for monomer and polymer synthesis. *Molecules* **2022**, *27*, 4071. [[CrossRef](#)]
76. Biddy, M.J.; Davis, R.; Humbird, D.; Tao, L.; Dowe, N.; Guarnieri, M.T.; Linger, J.G.; Karp, E.M.; Salvachúa, D.; Vardon, D.R.; et al. The techno-economic basis for coproduct manufacturing to enable hydrocarbon fuel production from lignocellulosic biomass. *ACS Sustain. Chem. Eng.* **2016**, *4*, 3196–3211. [[CrossRef](#)]
77. Oh, C.; Choi, E.H.; Choi, E.J.; Premkumar, T.; Song, C. Facile solid-state mechanochemical synthesis of eco-friendly thermoplastic polyurethanes and copolymers using a biomass-derived furan diol. *ACS Sustain. Chem. Eng.* **2020**, *8*, 4400–4406. [[CrossRef](#)]
78. Schmaltz, B.; Weil, T.; Müllen, K. Polyphenylene-based materials: Control of the electronic function by molecular and supramolecular complexity. *Adv. Mat.* **2009**, *21*, 1067–1078. [[CrossRef](#)]
79. Baumgarten, M.; Müllen, K. Chapter 6, Functional Polyphenylenes for Supramolecular Ordering and Application in Organic Electronics. In *Functional Supramolecular Architectures*; Samorì, P., Cacialli, F., Eds.; Wiley: Hoboken, NJ, USA, 2011; ISBN 9783527689897. [[CrossRef](#)]
80. Li, C.; Liu, M.; Pschirer, N.G.; Baumgarten, M.; Müllen, K. Polyphenylene-based materials for organic photovoltaics. *Chem. Rev.* **2010**, *110*, 6817–6855. [[CrossRef](#)]
81. Chang, Y.; Cao, H.; Feng, Q.; Wei, Y.; Bian, L.; Ling, H.; Lin, D.; Xie, L.; Huang, W. Organic semiconductors based on complex diarylfluorenes via Friedel-Crafts protocols of fluorenols. *Chin. Sci. Bull.* **2021**, *66*, 4268–4283. [[CrossRef](#)]
82. Lipton-Duffin, J.A.; Ivasenko, O.; Perepichka, D.F.; Rosei, F. Synthesis of polyphenylene molecular wires by surface-confined polymerization. *Small* **2009**, *5*, 592–597. [[CrossRef](#)]
83. Abe, M.; Yamamoto, T. Modification of soluble polyphenylene by Friedel–Crafts reactions: Introduction of benzyl and toluoyl groups to the polyphenylene and effects of the introduced group on optical properties of the polymer. *Synth. Met.* **2006**, *156*, 1118–1122. [[CrossRef](#)]
84. Vogt, C.G.; Grätz, S.; Lukin, S.; Halasz, I.; Etter, M.; Evans, J.D.; Borchardt, L. Direct Mechano catalysis: Palladium as milling media and catalyst in the mechanochemical Suzuki polymerization. *Angew. Chem. Int. Ed.* **2019**, *58*, 18942–18947. [[CrossRef](#)] [[PubMed](#)]
85. Grätz, S.; Wolfrum, B.; Borchardt, L. Mechanochemical Suzuki polycondensation—From linear to hyperbranched polyphenylenes. *Green Chem.* **2017**, *19*, 2973–2979. [[CrossRef](#)]
86. Skotheim, T.A.; Elsenbaumer, R.L.; Reynolds, J.R. (Eds.) *Handbook of Conducting Polymer Second Edition Revises and Expanded*; Marcel Dekker Inc.: New York, NY, USA, 1998.
87. Pal, B.; Yen, W.; Yang, J.; Su, W. Substituent effect on the optoelectronic properties of alternating fluorene-thiophene copolymers. *Macromolecules* **2007**, *40*, 8189–8194. [[CrossRef](#)]
88. Inagi, S.; Hayashi, S.; Hosaka, K.; Fuchigami, T. Facile functionalization of a thiophene-fluorene alternating copolymer via electrochemical polymer reaction. *Macromolecules* **2009**, *42*, 3881–3883. [[CrossRef](#)]
89. Ego, C.; Marsitzky, D.; Becker, S.; Zhang, J.; Grimsdale, A.C.; Müllen, K.; MacKenzie, J.D.; Silva, C.; Friend, R.H. Attaching perylene dyes to polyfluorene: Three simple, efficient methods for facile color tuning of light-emitting polymers. *J. Am. Chem. Soc.* **2003**, *125*, 437–443. [[CrossRef](#)]
90. Coffin, R.C.; Peet, J.; Rogers, J.; Bazan, G.C. Streamlined microwave-assisted preparation of narrow-bandgap conjugated polymers for high-performance bulk heterojunction solar cells. *Nat. Chem.* **2009**, *1*, 657–661. [[CrossRef](#)]
91. Zhang, Y.; Tajima, K.; Hirota, K.; Hashimoto, K. Synthesis of all-conjugated diblock copolymers by quasi-living polymerization and observation of their microphase separation. *J. Am. Chem. Soc.* **2008**, *130*, 7812–7813. [[CrossRef](#)]
92. Rothe, C.; Galbrecht, F.; Scherf, U.; Monkman, A. The β -phase of poly(9,9-dioctylfluorene) as a potential system for electrically pumped organic lasing. *Adv. Mater.* **2006**, *18*, 2137–2140. [[CrossRef](#)]
93. Grell, M.; Bradley, D.D.C.; Ungar, G.; Hill, J.; Whitehead, K.S. Interplay of physical structure and photophysics for a liquid crystalline polyfluorene. *Macromolecules* **1999**, *32*, 5810–5817. [[CrossRef](#)]
94. Hayashi, S.; Inagi, S.; Fuchigami, T. Macrostructural order and optical properties of polyfluorene-based polymer films. *Polym. J.* **2010**, *42*, 772–775. [[CrossRef](#)]
95. Neher, D. Polyfluorene homopolymers: Conjugated liquid-crystalline polymers for bright blue emission and polarized electroluminescence. *Macromol. Rapid Commun.* **2001**, *22*, 1365–1385. [[CrossRef](#)]
96. Scherf, U.; List, E.J.W. Semiconducting polyfluorenes—towards reliable structure–property relationships. *Adv. Mater.* **2002**, *14*, 477–487. [[CrossRef](#)]

97. Knaapila, M.; Monkman, A.P. Methods for controlling structure and photophysical properties in polyfluorene solutions and gels. *Adv. Mater.* **2013**, *25*, 1090–1108. [[CrossRef](#)]
98. Nirmani, L.P.T.; Pary, F.F.; Nelson, T.L. Mechanochemical Suzuki polymerization for the synthesis of polyfluorenes. *Green Chem. Lett. Rev.* **2022**, *15*, 863–868. [[CrossRef](#)]
99. Bhadra, J.; Alkareem, A.; Al-Thani, N. A review of advances in the preparation and application of polyaniline based thermoset blends and composites. *J. Polym. Res.* **2020**, *27*, 122. [[CrossRef](#)]
100. Gómez, I.J.; Sulleiro, M.V.; Mantione, D.; Alegret, N. Carbon nanomaterials embedded in conductive polymers: A state of the art. *Polymers* **2021**, *13*, 745. [[CrossRef](#)]
101. Beygisangchin, M.; Rashid, S.A.; Shafie, S.; Sadrolhosseini, A.R.; Lim, H.N. Preparations, properties, and applications of polyaniline and polyaniline thin films—A review. *Polymers* **2021**, *13*, 2003. [[CrossRef](#)]
102. Jaymand, M. Recent progress in chemical modification of polyaniline. *Prog. Polym. Sci.* **2013**, *38*, 1287–1306. [[CrossRef](#)]
103. Liao, G. Green preparation of sulfonated polystyrene/polyaniline/silver composites with enhanced anticorrosive properties. *Int. J. Chem.* **2018**, *10*, 81. [[CrossRef](#)]
104. Lu, X.; Zhang, W.; Wang, C.; Wen, T.C.; Wei, Y. One-dimensional conducting polymer nanocomposites: Synthesis, properties and applications. *Prog. Polym. Sci.* **2011**, *36*, 671–712. [[CrossRef](#)]
105. Zhou, Z.H.; Zhang, X.X.; Tian, D.; Xiong, R.; Lu, C.H. Solvent free synthesis of polyaniline with improved molecular weight through solid state mechanochemical milling at ambient temperature. *Mater. Res. Innov.* **2013**, *17*, 84–91. [[CrossRef](#)]
106. Šeděnková, I.; Konyushenko, E.N.; Stejskal, J.; Trchová, M.; Prokeš, J. Solid-state oxidation of anilinium chloride with various oxidants. *Synth. Met.* **2011**, *161*, 1353–1360. [[CrossRef](#)]
107. Posudievsky, O.Y.; Goncharuk, O.A.; Barillé, R.; Pokhodenko, V.D. Structure-property relationship in mechanochemically prepared polyaniline. *Synth. Met.* **2010**, *160*, 462–467. [[CrossRef](#)]
108. Huang, J.; Moore, J.A.; Acquaye, J.H.; Kaner, R.B. Mechanochemical route to the conducting polymer polyaniline. *Macromolecules* **2005**, *38*, 317–321. [[CrossRef](#)]
109. Bhandari, S.; Khastgir, D. Template-free solid state synthesis of ultra-long hairy polyaniline nanowire supercapacitor. *Mater. Lett.* **2014**, *135*, 202–205. [[CrossRef](#)]
110. Pandian, P.; Kalimuthu, R.; Arumugam, S.; Kannaiyan, P. Solid phase mechanochemical synthesis of poly(o-anisidine) protected silver nanoparticles for electrochemical dopamine sensor. *Mater. Today Commun.* **2021**, *26*, 102191. [[CrossRef](#)]
111. Barbero, C.A.; Acevedo, D.F. Mechanochemical synthesis of polyanilines and their nanocomposites: A critical review. *Polymers* **2023**, *15*, 133. [[CrossRef](#)]
112. Jiang, Y.; Ji, J.; Huang, L.; He, C.; Zhang, J.; Wang, X.; Yang, Y. One-pot mechanochemical exfoliation of graphite and in situ polymerization of aniline for the production of graphene/polyaniline composites for high-performance supercapacitors. *RSC Adv.* **2020**, *10*, 44688. [[CrossRef](#)]
113. Lou, Y.-C.; Qi, S.-C.; Xue, D.-M.; Gu, C.; Zhou, R.; Liu, X.-Q.; Sun, L.-B. Solvent-free synthesis of n-containing polymers with high cross-linking degree to generate n-doped porous carbons for high-efficiency CO₂ capture. *Chem. Eng. J.* **2020**, *399*, 125845. [[CrossRef](#)]
114. Das, S.; Heasman, P.; Ben, T.; Qiu, S. Porous organic materials: Strategic design and structure–function correlation. *Chem. Rev.* **2016**, *117*, 1515–1563. [[CrossRef](#)]
115. Xu, Y.; Jin, S.; Xu, H.; Nagai, A.; Jiang, D. Conjugated microporous polymers: Design, synthesis and application. *Chem. Soc. Rev.* **2013**, *42*, 8012–8031. [[CrossRef](#)]
116. Wang, Z.; Luo, X.; Zheng, B.; Huang, L.; Hang, C.; Jiao, Y.; Cao, X.; Zeng, W.; Yun, R. Highly selective carbon dioxide capture and cooperative catalysis of a water-stable acylamide-functionalized metal–organic framework. *Eur. J. Inorg. Chem.* **2018**, *2018*, 1309–1314. [[CrossRef](#)]
117. Yoon, M.; Srirambalaji, R.; Kim, K. Homochiral metal–organic frameworks for asymmetric heterogeneous catalysis. *Chem. Rev.* **2011**, *112*, 1196–1231. [[CrossRef](#)]
118. Xu, S.; Song, K.; Li, T.; Tan, B. Palladium catalyst coordinated in knitting N-heterocyclic carbene porous polymers for efficient Suzuki–Miyaura coupling reactions. *J. Mater. Chem. A* **2015**, *3*, 1272–1278. [[CrossRef](#)]
119. Pan, L.; Xu, M.-Y.; Feng, L.-J.; Chen, Q.; He, Y.-J.; Han, B.-H. Conjugated microporous polycarbazole containing tris (2-phenylpyridine) iridium (III) complexes: Phosphorescence, porosity, and heterogeneous organic photocatalysis. *Polym. Chem.* **2016**, *7*, 2299–2307. [[CrossRef](#)]
120. Zhao, X.; Zhang, S.; Yan, J.; Li, L.; Wu, G.; Shi, W.; Yang, G.; Guan, N.; Cheng, P. Polyoxometalate-based metal–organic frameworks as visible-light-induced photocatalysts. *Inorg. Chem.* **2018**, *57*, 5030–5037. [[CrossRef](#)]
121. Zheng, B.; Liu, H.; Wang, Z.; Yu, X.; Yi, P.; Bai, J. Porous NbO-type metal–organic framework with inserted acylamide groups exhibiting highly selective CO₂ capture. *CrystEngComm* **2013**, *15*, 3517–3520. [[CrossRef](#)]
122. Lu, Z.; Du, L.; Zheng, B.; Bai, J.; Zhang, M.; Yun, R. A highly porous agw-type metal–organic framework and its CO₂ and H₂ adsorption capacity. *CrystEngComm* **2013**, *15*, 9348–9351. [[CrossRef](#)]
123. Du, N.; Park, H.B.; Robertson, G.P.; Dal-Cin, M.M.; Visser, T.; Scoles, L.; Guiver, M.D. Polymer nanosieve membranes for CO₂-capture applications. *Nat. Mater.* **2011**, *10*, 372–375. [[CrossRef](#)]
124. Li, G.; Liu, Q.; Xia, B.; Huang, J.; Li, S.; Guan, Y.; Zhou, H.; Liao, B.; Zhou, Z.; Liu, B. Synthesis of stable metal-containing porous organic polymers for gas storage. *Eur. Polym. J.* **2017**, *91*, 242–247. [[CrossRef](#)]

125. Zheng, B.; Huang, L.; Cao, X.; Shen, S.; Cao, H.; Hang, C.; Zeng, W.; Wang, Z. A highly porous acylamide decorated MOF-505 analogue exhibiting high and selective CO₂ gas uptake capability. *CrystEngComm* **2018**, *20*, 1874–1881. [[CrossRef](#)]
126. Zheng, B.; Luo, X.; Wang, Z.; Zhang, S.; Yun, R.; Huang, L.; Zeng, W.; Liu, W. An unprecedented water stable acylamide-functionalized metal–organic framework for highly efficient CH₄/CO₂ gas storage/separation and acid–base cooperative catalytic activity. *Inorg. Chem. Front.* **2018**, *5*, 2355–2363. [[CrossRef](#)]
127. Sun, H.; Ren, D.; Kong, R.; Wang, D.; Jiang, H.; Tan, J.; Wu, D.; Chen, S.; Shen, B. Tuning 1-hexene/n-hexane adsorption on MOF-74 via constructing Co-Mg bimetallic frameworks. *Microporous Mesoporous Mater.* **2019**, *284*, 151–160. [[CrossRef](#)]
128. Novoa-Cid, M.; Melillo, A.; Ferrer, B.; Alvaro, M.; Baldovi, H.G. Photocatalytic water splitting promoted by 2d and 3d porphyrin covalent organic polymers synthesized by Suzuki-Miyaura carbon-carbon coupling. *Nanomaterials* **2022**, *12*, 3197. [[CrossRef](#)]
129. Martín, C.F.; Stöckel, E.; Clowes, R.; Adams, D.J.; Cooper, A.I.; Pis, J.J.; Rubiera, F.; Pevida, C. Hypercrosslinked organic polymer networks as potential adsorbents for pre-combustion CO₂ capture. *J. Mater. Chem.* **2011**, *21*, 5475–5483. [[CrossRef](#)]
130. Kuhn, P.; Antonietti, M.; Thomas, A. Porous, covalent triazine-based frameworks prepared by ionothermal synthesis. *Angew. Chem. Int. Ed.* **2008**, *47*, 3450–3453. [[CrossRef](#)]
131. Pandey, P.; Katsoulidis, A.P.; Eryazici, I.; Wu, Y.; Kanatzidis, M.G.; Nguyen, S.T. Imine-linked microporous polymer organic frameworks. *Chem. Mater.* **2010**, *22*, 4974–4979. [[CrossRef](#)]
132. Ritter, N.; Senkowska, I.; Kaskel, S.; Weber, J. Towards chiral microporous soluble polymers—Binaphthalene-based polyimides. *Macromol. Rapid Commun.* **2011**, *32*, 438–443. [[CrossRef](#)]
133. Tan, L.; Tan, B. Hypercrosslinked porous polymer materials: Design, synthesis, and applications. *Chem. Soc. Rev.* **2017**, *46*, 3322–3356. [[CrossRef](#)]
134. Grätz, S.; Zink, S.; Krafczyk, H.; Rose, M.; Borchardt, L. Mechanochemical synthesis of hyper-crosslinked polymers: Influences on their pore structure and adsorption behaviour for organic vapors. *Beilstein J. Org. Chem.* **2019**, *15*, 1154–1161. [[CrossRef](#)]
135. Giri, A.; Biswas, S.; Hussain, M.W.; Dutta, T.K.; Patra, A. Nanostructured Hypercrosslinked Porous Organic Polymers: Morphological Evolution and Rapid Separation of Polar Organic Micropollutants. *ACS Appl. Mater. Interfaces.* **2022**, *14*, 7369–7381. [[CrossRef](#)]
136. Grätz, S.; Oltermann, M.; Troschke, E.; Paasch, S.; Krause, S.; Brunner, E.; Borchardt, L. Solvent-free synthesis of a porous thiophene polymer by mechanochemical oxidative polymerization. *J. Mater. Chem. A* **2018**, *6*, 21901–21905. [[CrossRef](#)]
137. Konnert, L.; Gaultier, A.; Lamaty, F.; Martinez, J.; Colacino, E. Solventless synthesis of *N*-protected amino acids in a ball mill. *ACS Sustain. Chem. Eng.* **2013**, *1*, 1186–1191. [[CrossRef](#)]
138. Chen, Q.; Liu, D.-P.; Luo, M.; Feng, L.-J.; Zhao, Y.-C.; Han, B.-H. Nitrogen-containing microporous conjugated polymers via carbazole-based oxidative coupling polymerization: Preparation, porosity, and gas uptake. *Small* **2014**, *10*, 308–315. [[CrossRef](#)]
139. Zhu, X.; Tian, C.; Jin, T.; Browning, K.L.; Sacci, R.L.; Veith, G.M.; Dai, S. Solid-state synthesis of conjugated nanoporous polycarbazoles. *ACS Macro Lett.* **2017**, *6*, 1056–1059. [[CrossRef](#)]
140. Krusenbaum, A.; Geisler, J.; Kraus, F.J.L.; Grätz, S.; Höfler, M.V.; Gutmann, T.; Borchardt, L. The mechanochemical Friedel-Crafts polymerization as a solvent-free cross-linking approach toward microporous polymers. *J. Polym. Sci.* **2022**, *60*, 62–71. [[CrossRef](#)]
141. McKeown, N.B.; Budd, P.M. Polymers of intrinsic microporosity (PIMs): Organic materials for membrane separations, heterogeneous catalysis and hydrogen storage. *Chem. Soc. Rev.* **2006**, *35*, 675–683. [[CrossRef](#)]
142. McKeown, N.B.; Budd, P.M.; Msayib, K.J.; Ghanem, B.S.; Kingston, H.J.; Tattershall, C.E.; Makhseed, S.; Reynolds, K.J.; Fritsch, D. Polymers of Intrinsic Microporosity (PIMs): Bridging the Void between Microporous and Polymeric Materials. *Chem. Eur. J.* **2005**, *11*, 2610–2620. [[CrossRef](#)]
143. Zhu, X.; Hua, Y.; Tian, C.; Abney, C.W.; Zhang, P.; Jin, T.; Liu, G.; Browning, K.L.; Sacci, R.L.; Veith, G.M.; et al. Accelerating membrane-based CO₂ separation by soluble nanoporous polymer networks produced by mechanochemical oxidative coupling. *Angew. Chem. Int. Ed.* **2018**, *57*, 2816–2821. [[CrossRef](#)]
144. Ma, H.; Ren, H.; Meng, S.; Sun, F.; Zhu, G. Novel porphyrinic porous organic frameworks for high performance separation of small hydrocarbons. *Sci. Rep.* **2013**, *3*, 2611. [[CrossRef](#)] [[PubMed](#)]
145. Kuhn, P.; Forget, A.; Su, D.; Thomas, A.; Antonietti, M. From microporous regular frameworks to mesoporous materials with ultrahigh surface area: Dynamic reorganization of porous polymer networks. *J. Am. Chem. Soc.* **2008**, *130*, 13333–13337. [[CrossRef](#)] [[PubMed](#)]
146. Kuhn, P.; Thomas, A.; Antonietti, M. Toward tailorable porous organic polymer networks: A high-temperature dynamic polymerization scheme based on aromatic nitriles. *Macromolecules* **2009**, *42*, 319–326. [[CrossRef](#)]
147. Liao, L.; Li, M.; Yin, Y.; Chen, J.; Zhong, Q.; Du, R.; Liu, S.; He, Y.; Fu, W.; Zeng, F. Advances in the Synthesis of Covalent Triazine Frameworks. *ACS Omega* **2023**, *8*, 4527–4542. [[CrossRef](#)]
148. Ren, S.; Bojdys, M.J.; Dawson, R.; Laybourn, A.; Khimiyak, Y.Z.; Adams, D.J.; Cooper, A.I. Porous, fluorescent, covalent triazine-based frameworks via room-temperature and microwave-assisted synthesis. *Adv. Mater.* **2012**, *24*, 2357–2361. [[CrossRef](#)]
149. Kuecken, S.; Schmidt, J.; Zhi, L.; Thomas, A. Conversion of amorphous polymer networks to covalent organic frameworks under ionothermal conditions: A facile synthesis route for covalent triazine frameworks. *J. Mater. Chem. A* **2015**, *3*, 24422–24427. [[CrossRef](#)]
150. Hao, L.; Ning, J.; Luo, B.; Wang, B.; Zhang, Y.; Tang, Z.; Yang, J.; Thomas, A.; Zhi, L. Structural evolution of 2D microporous covalent triazine-based framework toward the study of high-performance supercapacitors. *J. Am. Chem. Soc.* **2015**, *137*, 219–225. [[CrossRef](#)]

151. Liao, H.; Ding, H.; Li, B.; Ai, X.; Wang, C. Covalent-organic frameworks: Potential host materials for sulfur impregnation in lithium–sulfur batteries. *J. Mater. Chem. A* **2014**, *2*, 8854–8858. [[CrossRef](#)]
152. Talapaneni, S.N.; Hwang, T.H.; Je, S.H.; Buyukcakir, O.; Choi, J.W.; Coskun, A. Elemental-Sulfur-Mediated Facile Synthesis of a Covalent Triazine Framework for High-Performance Lithium–Sulfur Batteries. *Angew. Chem. Int. Ed.* **2016**, *55*, 3106–3111. [[CrossRef](#)]
153. Borchardt, L.; Oschatz, M.; Kaskel, S. Carbon Materials for Lithium Sulfur Batteries—Ten Critical Questions. *Chem. Eur. J.* **2016**, *22*, 7324–7351. [[CrossRef](#)]
154. Dey, S.; Bhunia, A.; Esquivel, D.; Janiak, C. Covalent triazine-based frameworks (CTFs) from triptycene and fluorene motifs for CO₂ adsorption. *J. Mater. Chem. A* **2016**, *4*, 6259–6263. [[CrossRef](#)]
155. Hug, S.; Stegbauer, L.; Oh, H.; Hirscher, M.; Lotsch, B.V. Nitrogen-rich covalent triazine frameworks as high-performance platforms for selective carbon capture and storage. *Chem. Mater.* **2015**, *27*, 8001–8010. [[CrossRef](#)]
156. Zhao, Y.; Yao, K.X.; Teng, B.; Zhang, T.; Han, Y. A perfluorinated covalent triazine-based framework for highly selective and water-tolerant CO₂ capture. *Energy Environ. Sci.* **2013**, *6*, 3684–3692. [[CrossRef](#)]
157. Troschke, E.; Grätz, S.; Lübken, T.; Borchardt, L. Mechanochemical Friedel–Crafts alkylation—A sustainable pathway towards porous organic polymers. *Angew. Chem.* **2017**, *129*, 6963–6967. [[CrossRef](#)]
158. Yuan, R.; Yan, Z.; Shaga, A.; He, H. Solvent-free mechanochemical synthesis of a carbazole-based porous organic polymer with high CO₂ capture and separation. *J. Solid State Chem.* **2020**, *287*, 121327. [[CrossRef](#)]
159. Wang, S.; Dai, T.; Lu, Y.; Chen, Q.; Feng, L.; Sui, Z. Fullerene-bearing porous polymer via ball-milling approach and its palladium composite for catalytic deallylation. *Microporous Mesoporous Mater.* **2020**, *302*, 110187. [[CrossRef](#)]
160. Giacalone, F.; Martín, N. Fullerene polymers: Synthesis and properties. *Chem. Rev.* **2006**, *106*, 5136–5190. [[CrossRef](#)]
161. Balch, A.L.; Winkler, K. Two-component polymeric materials of fullerenes and the transition metal complexes: A bridge between metal–organic frameworks and conducting polymers. *Chem. Rev.* **2016**, *116*, 3812–3882. [[CrossRef](#)]
162. Wang, C.; Guo, Z.-X.; Fu, S.; Wu, W.; Zhu, D. Polymers containing fullerene or carbon nanotube structures. *Prog. Polym. Sci.* **2004**, *29*, 1079–1141. [[CrossRef](#)]
163. Kang, H.; Cho, C.-H.; Cho, H.-H.; Kang, T.E.; Kim, H.J.; Kim, K.-H.; Yoon, S.C.; Kim, B.J. Controlling number of indene solubilizing groups in multiadduct fullerenes for tuning optoelectronic properties and open-circuit voltage in organic solar cells. *ACS Appl. Mater. Interfaces* **2012**, *4*, 110–116. [[CrossRef](#)]
164. Pan, Q.; Xu, Z.; Deng, S.; Zhang, F.; Li, H.; Cheng, Y.; Wei, L.; Wang, J.; Zhou, B. A Mechanochemically synthesized porous organic polymer derived CQD/chitosan–graphene composite film electrode for electrochemiluminescence determination of dopamine. *RSC Adv.* **2019**, *9*, 39332–39337. [[CrossRef](#)] [[PubMed](#)]
165. Ohura, T.; Tsutaki, Y.; Sakaguchi, M. Novel synthesis of cellulose-based diblock copolymer of poly(hydroxyethyl methacrylate) by mechanochemical reaction. *Sci. World J.* **2014**, *2014*, 127506. [[CrossRef](#)] [[PubMed](#)]
166. Ohn, N.; Kim, J.G. Mechanochemical post-polymerization modification: Solvent-free solid-state synthesis of functional polymers. *ACS Macro Lett.* **2018**, *7*, 561–565. [[CrossRef](#)] [[PubMed](#)]
167. Han, S.; Lee, J.; Jung, E.; Park, S.; Sagawa, A.; Shibasaki, Y.; Kim, B.-S. Mechanochemical drug conjugation via pH-responsive imine linkage for polyether prodrug micelles. *ACS Appl. Bio Mater.* **2021**, *4*, 2465–2474. [[CrossRef](#)] [[PubMed](#)]
168. Malca, M.Y.; Ferko, P.-O.; Friščić, T.; Moores, A. Solid-state mechanochemical ω functionalization of poly(ethylene glycol). *Beilstein J. Org. Chem.* **2017**, *13*, 1963–1968. [[CrossRef](#)]
169. Ashlin, M.; Hobbs, C.E. Post-polymerization thiol substitutions facilitated by mechanochemistry. *Macromol. Chem. Phys.* **2019**, *220*, 1900350. [[CrossRef](#)]
170. Lee, G.S.; Lee, H.W.; Lee, H.S.; Do, T.; Do, J.-L.; Lim, J.; Peterson, G.I.; Friščić, T.; Kim, J.G. Mechanochemical ring-opening metathesis polymerization: Development, scope, and mechano-exclusive polymer synthesis. *Chem. Sci.* **2022**, *13*, 11496–11505. [[CrossRef](#)]
171. Do, J.-L.; Mottillo, C.; Tan, D.; Štrukil, V.; Friščić, T. Mechanochemical ruthenium-catalyzed olefin metathesis. *J. Am. Chem. Soc.* **2015**, *137*, 2476–2479. [[CrossRef](#)]
172. Park, J.; Murayama, S.; Osaki, M.; Yamaguchi, H.; Harada, A.; Matsuba, G.; Takashima, Y. Extremely rapid self-healable and recyclable supramolecular materials through planetary ball milling and host–guest interactions. *Adv. Mat.* **2020**, *32*, 2002008. [[CrossRef](#)]
173. Kubota, K.; Toyoshima, N.; Miura, D.; Jiang, J.; Maeda, S.; Jin, M.; Ito, H. Introduction of a luminophore into generic polymers via mechanoradical coupling with a prefluorescent reagent. *Angew. Chem. Int. Ed.* **2021**, *60*, 16003–16008. [[CrossRef](#)]
174. Chung, W.J.; Griebel, J.J.; Kim, E.T.; Yoon, H.; Simmonds, A.G.; Ji, H.J.; Dirlam, P.T.; Glass, R.S.; Wie, J.J.; Nguyen, N.A.; et al. The use of elemental sulfur as an alternative feedstock for polymeric materials. *Nat. Chem.* **2013**, *5*, 518–524. [[CrossRef](#)]
175. Yan, P.; Zhao, W.; McBride, F.; Cai, D.; Dale, J.; Hanna, V.; Hasell, T. Mechanochemical synthesis of inverse vulcanized polymers. *Nat. Commun.* **2022**, *13*, 4824. [[CrossRef](#)]
176. Cavalieri, F.; Padella, F. Development of composite materials by mechanochemical treatment of post-consumer plastic waste. *Waste Manag.* **2002**, *22*, 913–916. [[CrossRef](#)]
177. Baheti, V.; Abbasi, R.; Militky, J. Ball milling of jute fiber wastes to prepare nanocellulose. *World J. Eng.* **2012**, *9*, 45–50. [[CrossRef](#)]
178. Razzak, S.A.-A.; Lofgren, E.A.; Jabarin, S.A. End-group determination in poly(ethylene terephthalate) by infrared spectroscopy. *Polym. Int.* **2002**, *51*, 174–182.

179. Takacs, L.; McHenry, J.S. Temperature of the milling balls in shaker and planetary mills. *J. Mater. Sci.* **2006**, *41*, 5246–5249. [[CrossRef](#)]
180. Kubota, K.; Ito, H. Mechanochemical Cross-Coupling Reactions. *Trends Chem.* **2020**, *2*, 1066–1081. [[CrossRef](#)]
181. Post, W.; Susa, A.; Blaauw, R.; Molenveld, K.; Knoop, R.J.I. A review on the potential and limitations of recyclable thermosets for structural applications. *Polym. Rev.* **2020**, *60*, 359–388. [[CrossRef](#)]
182. Worch, J.C.; Dove, A.P. 100th anniversary of macromolecular science viewpoint: Toward catalytic chemical recycling of waste (and future) plastics. *ACS Macro Lett.* **2020**, *9*, 1494–1506. [[CrossRef](#)]
183. Qin, B.; Liu, S.; Huang, Z.; Zeng, L.; Xu, J.-F.; Zhang, X. Closed-loop chemical recycling of cross-linked polymeric materials based on reversible amidation chemistry. *Nat. Commun.* **2022**, *13*, 7595. [[CrossRef](#)]
184. Hussain, Z.; Khan, K.M.; Hussain, K. Microwave–metal interaction pyrolysis of polystyrene. *J. Anal. Appl. Pyrolysis* **2010**, *89*, 39–43. [[CrossRef](#)]
185. Bartoli, M.; Rosi, L.; Frediani, M.; Undri, A.; Frediani, P. Depolymerization of polystyrene at reduced pressure through a microwave assisted pyrolysis. *J. Anal. Appl. Pyrolysis* **2015**, *113*, 281–287. [[CrossRef](#)]
186. Onwudili, J.A.; Insura, N.; Williams, P.T. Composition of products from the pyrolysis of polyethylene and polystyrene in a closed batch reactor: Effects of temperature and residence time. *J. Anal. Appl. Pyrolysis* **2009**, *86*, 293–303. [[CrossRef](#)]
187. Undri, A.; Frediani, M.; Rosi, L.; Frediani, P. Reverse polymerization of waste polystyrene through microwave assisted pyrolysis. *J. Anal. Appl. Pyrolysis* **2014**, *105*, 35–42. [[CrossRef](#)]
188. Faravelli, T.; Pincioli, M.; Pisano, F.; Bozzano, G.; Dente, M.; Ranzi, E. Thermal degradation of polystyrene. *J. Anal. Appl. Pyrolysis* **2001**, *60*, 103–121. [[CrossRef](#)]
189. Štrukil, V. Highly efficient solid-state hydrolysis of waste polyethylene terephthalate by mechanochemical milling and vapor-assisted aging. *ChemSusChem* **2021**, *14*, 330–338. [[CrossRef](#)]
190. Balema, V.P.; Hlova, I.Z.; Carnahan, S.L.; Seyed, M.; Dolotko, O.; Rossini, A.J.; Luzinov, I. Depolymerization of polystyrene under ambient conditions. *New J. Chem.* **2021**, *45*, 2935–2938. [[CrossRef](#)]

Disclaimer/Publisher’s Note: The statements, opinions and data contained in all publications are solely those of the individual author(s) and contributor(s) and not of MDPI and/or the editor(s). MDPI and/or the editor(s) disclaim responsibility for any injury to people or property resulting from any ideas, methods, instructions or products referred to in the content.